

DESIGN AND ANALYSIS OF VEHICLE MOUNTED ON SOLAR AND WIND POWER SYSTEM

*THESIS SUBMITTED IN PARTIAL FULFILMENTS OF THE REQUIREMENT FOR THE
DEGREE OF MASTER OF ENGINEERING IN AUTOMOBILE ENGINEERING UNDER
FACULTY OF ENGINEERING AND TECHNOLOGY*

Submitted by

AJAY DEY

Class Roll No.: 002111204009

Examination Roll No.: M4AUT23005

Registration No.: 160303 of 2021-22

Academic Session: 2021-2023

Under the guidance of

Prof. Nipu Modak

Department of Mechanical Engineering

Jadavpur University

DEPARTMENT OF MECHANICAL ENGINEERING

JADAVPUR UNIVERSITY

188, RAJA S.C. MULLICK ROAD, KOLKATA – 700 032

FACULTY OF ENGINEERING & TECHNOLOGY
DEPARTMENT OF MECHANICAL ENGINEERING
JADAVPUR UNIVERSITY
KOLKATA – 700 032

CERTIFICATE OF APPROVAL

The foregoing thesis, entitled “**DESIGN AND ANALYSIS OF VEHICLE MOUNTED ON SOLAR AND WIND POWER SYSTEM**” is hereby approved as a creditable study in the area of Automobile Engineering carried out and presented by Mr. Ajay Dey (Registration No.: 160303 of 2021-22) in a satisfactory manner to warrant its acceptance as a prerequisite to the degree for which it has been submitted. It is notified to be understood that by this approval, the undersigned do not necessarily endorse or approve any statement made, opinion expressed and conclusion drawn therein but approve the thesis only for the purpose for which it has been submitted.

Committee of final evaluation of thesis:

(Signature of Examiners)

FACULTY OF ENGINEERING & TECHNOLOGY
DEPARTMENT OF MECHANICAL ENGINEERING
JADAVPUR UNIVERSITY
KOLKATA – 700 032

CERTIFICATE OF RECOMMENDATION

This is to certify that the thesis entitled “**DESIGN AND ANALYSIS OF VEHICLE MOUNTED ON SOLAR AND WIND POWER SYSTEM**” is a bona fide work carried out by Mr. Ajay Dey under our supervision and guidance in partial fulfilment of the requirements for awarding the degree of Master of Engineering in Automobile Engineering under Department of Mechanical Engineering, Jadavpur University during the academic session 2021-2023.

THESIS SUPERVISOR

Prof. Nipu Modak

Professor

Department of Mechanical Engineering

Jadavpur University, Kolkata

Prof. Amit Karmakar

Head of the Department

Department of Mechanical Engineering

Jadavpur University, Kolkata

Prof. Saswati Mazumdar

Dean

Faculty Council of Engineering & Technology

Jadavpur University, Kolkata

DECLARATION OF ORIGINALITY AND COMPLIANCE OF ACADEMIC ETHICS

I hereby declare that the thesis entitled “**DESIGN AND ANALYSIS OF VEHICLE MOUNTED ON SOLAR AND WIND POWER SYSTEM**” contains literature survey and original research work by the undersigned candidate, as a part of his Master of Engineering in Automobile Engineering under the Department of Mechanical Engineering, studies during academic session 2021-2023.

All information in this document have been obtained and presented in accordance with the academic rules and ethical conduct.

I also declare that, as required by these rules of conduct, I have fully cited and referenced all the material and results that are not original to this work.

Name:	AJAY DEY
Class Roll Number:	002111204009
Examination Roll Number:	M4AUT23005
University Registration Number:	160303 of 2021-22

Date: /09/2023

(Signature)

AJAY DEY

Department of Mechanical Engineering
Jadavpur University, Kolkata – 700 032

Acknowledgements

First and foremost, I extend my deepest gratitude to my supervisor, Prof. Nipu Modak for his unwavering inspiration, motivation, and invaluable advice throughout my research. His encouragement and belief in my abilities enabled me to complete this research project. He guided me in the right direction to pinpoint my areas of strength and provided me with the psychological and informational support I needed to sign up for important courses on this topic, greatly expanding my knowledge. I am truly grateful to him for helping me reach this goal and for keeping me on the right path.

I would like to express my gratitude to Mr. Saumendra Nath Mishra, a PhD candidate who is also my senior, for his invaluable guidance on some aspects of this thesis. His advice resembled that of a caring older brother who stood by my side during the crucial portions of this research. When I went to him with a new problem involving my work, he always offered the best solutions. The ability to prepare this thesis was greatly aided by his insightful and priceless advice.

I want to separately thank my friends Ajit Das and Rittik Das for all of their support and help with the thesis.

Finally, I would like to express my sincere gratitude to my parents and other family members whose unwavering support and motivation were crucial to the accomplishment of this work.

Ajay Dey

Department of Mechanical Engineering
Jadavpur University, Kolkata – 700 032

Date: /09/2023

Abstract

This thesis aims to investigate the development and performance analysis of a four-wheeler car powered by renewable energy sources, specifically solar and wind energy. The research focuses on designing and implementing a sustainable transportation solution that can reduce reliance on fossil fuels and mitigate environmental impacts. The study includes the design and integration of solar panels and wind turbines into the car's architecture, along with evaluating the car's performance and efficiency. The findings of this research contribute to the growing field of sustainable transportation and provide valuable insights for the future development of renewable energy-powered vehicles. This paper discusses the technical aspects of designing a vehicle-mounted solar and wind power system, including considerations such as weight, size, power output, battery design, various control systems, and the connection of solar and wind power circuits. Additionally, the potential benefits of this system, such as improved fuel efficiency, reduce polluted gases and decrees energy dependency, are discussed. The paper concludes with a discussion of the analytical result of the experiment and the future scope of vehicle-mounted renewable energy systems and their possible effects on the automobile industry and the environment. For the wind and solar analysis ANSYS Workbench of CDF and CFX model and Steady-State-Thermal model has been used, respectively. MATLAB Simulink model is used for solar panel analysis. From the analysis find that the efficiency of solar panel is 15.18% and the power coefficient of the solar panel 0.26 at 60 km/h relative speed of wind and turbine blade with 25° tilt angle of blade. Total energy production for this hybrid electric vehicle system is 3.83 kW. A battery source of about 7.95 kW is required for the Maruti Eeco car to run for an hour at 60 km/h. Finally, it is claimed that this solar- and wind-powered hybrid electric vehicle can travel about 29 km per day without the help of a conventional energy system.

Table of Contents

Acknowledgements	v
Abstract.....	vi
Table of Contents	vii
List of Figures.....	ix
List of Tables.....	xi
Nomenclature and Subscripts	xii
Chapter 1 Introduction.....	1
1.1 Background and Motivation.....	1
1.2 Research Objectives	2
1.3 Scope and Limitations	2
1.4 Thesis Structure	2
Chapter 2 Literature Review	5
2.1 Solar Energy in Transportation.....	5
2.2 Wind Energy in Transportation	9
2.3 Integration of Solar and Wind Energy in Vehicle.....	13
Chapter 3 Methodology	16
3.1 System Architecture and Design	16
3.2 Solar Energy Integration	17
3.3 Wind Energy Integration	17
3.4 Testing and Validation	19
Chapter 4 Solar and Wind Energy Resource Assessment.....	21
4.1 Solar Energy Resource Assessment	21
4.2 Wind Energy Resource Assessment	25
4.3 Hybrid Electric Vehicle	25
4.4 Location Selection and Data Analysis.....	29
Chapter 5 Design and Integration of Solar and Wind Energy System	31
5.1 Solar Panel Design and Placement.....	31
5.1.1 Fundamentals of Photovoltaic Technology	31
5.1.2 Working Principle of Solar Panel (PV Cell) System.....	33
5.1.3 Monocrystalline PV Solar Cell	34
5.2 Wind Turbine Design and Placement	39

5.3	Integration of Solar and Wind Systems	43
5.4	Energy Conversion and Storage Systems	43
Chapter 6	Performance Analysis	45
6.1	Efficiency Analysis	45
6.2	Vehicle Performance Evaluation	45
6.2.1	Weather Condition on the Solar Panel System	46
6.2.2	Vehicle Speed effect on the Wind Turbine System	47
6.3	Energy Generation and Consumption Analysis	49
6.3.1	Solar Energy Generation	49
6.3.2	Solar Panel Voltage and Current Analysis	55
6.3.3	Wind Turbine Aerodynamic Analysis	56
6.3.4	Wind Turbine Power Calculation	61
6.3.5	Aerodynamic Analysis of the Vehicle	65
6.3.6	Required Power Calculation for Maruti Eeco Car at 60 Km/h	68
6.3.7	Battery Capacity Design	70
6.3.8	Cost and Weight Analysis	70
Chapter 7	Results & Discussion	72
7.1	Solar and Wind Energy Resource Assessment Results	72
7.2	Design and Integration Results	72
7.2.1	Solar Panel Result	72
7.3	Performance Analysis Results	74
7.4	Discussion of Findings	77
Chapter 8	Conclusion and Future Work	79
8.1	Summary of Findings	79
8.2	Contributions to Sustainable Transportation	79
8.3	Limitations and Challenges	80
8.4	Future Research Directions	80
References	82

List of Figures

Fig. 1: Schematic diagram of Solar and Wind Power System.....	16
Fig. 2: Schematic diagram of Wind Turbine Power Conversion.....	19
Fig. 3: Graph plot of Daily Global Irradiance and Temperature with 15 minutes interval from 18-21 July, 2023	23
Fig. 4: Graph plot of Solar Insolation (kWh/m^2) with months.....	23
Fig. 5: Graph plot of available Day Length varying with months.....	24
Fig. 6: Graph of 16 years average Solar Insolation and Temperature with respect to months.....	24
Fig. 7: Schematic diagram of different types of Hybrid Electric Vehicle	27
Fig. 8: Solar Panel and Wind Turbine position.....	30
Fig. 9: Working Process of Solar Panel	34
Fig. 10: Schematic diagram of Mono PERC Solar Panel.....	36
Fig. 11: Different layers of a Solar Panel	37
Fig. 12: Schematic diagram of Bifacial Mono PERC Solar Panel	39
Fig. 13: Schematic diagram of different parts of Wind Turbine.....	40
Fig. 14: Small Horizontal Axis Wind Turbine.....	42
Fig. 15: Wind Turbine Blade Chord Length Vs. Rotor Radius	43
Fig. 16: Drag and Lift Force at an Alpha Angle of Attack	47
Fig. 17: Solar Ray inclination Angle (θ°) on Earth Surface.....	51
Fig. 18: Graph of Solar Irradiance Vs. Hour Angle.....	55
Fig. 19: Solar Cell Electric Circuit	55
Fig. 20: Graph between Lift Coefficient and AOA (α°)	56
Fig. 21: Curve between Drag Coefficient and Lift Coefficient of Wind Turbine Blade	57
Fig. 22: Graph between Drag Coefficient and AOA	57

Fig. 23: a-Velocity Contour, b- Pressure Contour, c- Velocity with Streamline of wind turbine Blade Aerodynamic Analysis.....	58
Fig. 24: Curve between Power coefficient of Turbine with Tip Speed Ratio (λ).....	60
Fig. 25: a-Velocity Vector only rotation area of blade, b-Pressure Contour and c-Velocity Vector of the Wind Turbine Power Calculation.....	64
Fig. 26: Wind Turbine Power Coefficient Variation with AOA (α°)	64
Fig. 27: Graph Between Drag Coefficient of Vehicle and Vehicle Velocity	66
Fig. 28: Graph Between Drag force of Vehicle and Vehicle Velocity	66
Fig. 29: a-Pressure Contour, b-Velocity Contour and c-Velocity Vector of Vehicle Aerodynamic Analysis	67
Fig. 30: Final Vehicle Design	67
Fig. 31: At constant 25°C Temperature a-Output Current and b-Output Power Vs. Voltage Curve of Solar Panel at Different Solar Radiation Energy	72
Fig. 32: At constant 1000 W/m ² Irradiance a-Current and b-Power Vs. Voltage Curve of Solar Panel at Different Atmospheric Temperature	73
Fig. 33: MATLAB simulation model of Solar Panel Analysis.....	73
Fig. 34: a-Variation of Solar Panel Efficiency with Temperature at 1000 W/m ² Irradiance and b-Variation of Solar Panel Efficiency with Solar Irradiance at 25°C Temperature	74
Fig. 35: Value of Cl/Cd change with AOA(α°) at Different Vehicle Speed	75
Fig. 36: Wind Turbine Output Power with Relative Velocity between vehicle and wind at Different AOA.....	76
Fig. 37: Curve of Wind Turbine Power Vs. Wind Velocity	77

List of Tables

Table 1: Validation report of Solar and Wind Power System.....	20
Table 2: Horizontal Axis Wind Turbine Blade Design Parameter	42
Table 3: Number of days variation with date	50
Table 4: Climate correction factors at different season of Year	53
Table 5: Power output from Wind Turbine at 05° AOA.....	61
Table 6: Power output from Wind Turbine at 10° AOA.....	62
Table 7: Power output from Wind Turbine at 15° AOA.....	62
Table 8: Power output from Wind Turbine at 20° AOA.....	62
Table 9: Power output from Wind Turbine at 25° AOA.....	63
Table 10: Power output from Wind Turbine at 30° AOA.....	63
Table 11: Power output from Wind Turbine at 40° AOA.....	63
Table 12: Power output from Wind Turbine at 50° AOA.....	63
Table 13: Specification of Maruti Eeco 7-Seater Car	68
Table 14: Components Details of Designed Vehicles	70
Table 15: Details of removed component of Vehicle	71
Table 16: Table of Wind and Solar System Simulation and Analysis Result.....	77

Nomenclature and Subscripts

AR	Aspect ratio
a	Acceleration of vehicle
A_f	Frontal area of the vehicle
A_s	Surface area of solar panel
A_w	Swept area of wind turbine
α , AOA	Angle of attack of wind on wind-turbine blade
β	Pitch angle of wind turbine
β	Solar panel tilt angle
C	Blade cord length
C_d	Drag coefficient
C_L	Lift coefficient
C_p	Power coefficient of wind turbine
D_d	Drag force
D_L	Lift force
D_{rim}	Diameter of wheel rim
D_{tyre}	Diameter of wheel
δ	Solar declination angle
E_s	Solar panel produces energy
F	Draf force of vehicle
F_T	Total tractive force of vehicle
F_a	Acceleration resistance force of vehicle
F_g	Grade resistance force of vehicle
F_r	Rolling resistance force of vehicle
F_w	Aerodynamic force of vehicle
H	Annual average solar radiation on tilted panels
I	Current
I_{SC}	Solar radiation energy constant
m_i	Inertial vehicle mass
N	Rotation of wheel
N_b	Efficiency of bearings

N_g	Efficiency of gearbox
η_g	Efficiency of generator
η_s	Efficiency of solar panel
θ	Solar ray incidence angle
ϕ	Latitude
PR	Solar panel performance ratio
P_e	Output Electric power from wind
P_T	Total power required to run the vehicle
P_w	Available wind power of wind turbine at a velocity
ρ	Air density
r	Blade radius
T_{cell}	Average temperature of solar cell
τ_b	Atmospheric transmittance
μ_r	Rolling resistance coefficient of vehicle
V	Relative velocity between wind and vehicle
V	Volts
v	Wind velocity
W	Relative air speed
W	Sectional width of tyre
W_T	Total weight of vehicle
ω	Hour angle
ω	Angular velocity of wheel
λ	Wind turbine blade tip speed ratio
Z	Zenith angle

Chapter 1

Introduction

1.1 Background and Motivation

Due to the limitation of fossil fuels and concerns over global warming, the wind energy and solar energy technology has been developed greatly and become together a mature technology in the renewable energy field. Energy and environmental issues are among the most important problems of public concern. As fossil fuel deposits are depleted and our environment is degraded. It is important for society to wane its addiction off fossil fuels and transition to more sustainable forms of energy such as renewable sources of energy, form of energy that can be recovered in a human time scale such as solar, wind. In our society, the source of maximum greenhouse gasses mainly carbon dioxide (CO_2) and others harmful gasses are commercial vehicles. For this reason, we are more interested in the used of electric vehicles with renewable energy sources likes wind energy, solar energy and etc. Electric Vehicles are completely pollutions free. Wind and solar energy may be one of the alternative solutions to overcome energy shortage and to reduce greenhouse gaseous emission. Using electric cars in cities can significantly improve the air quality there.

However, the new technology provides a solution by allowing the cars to charge while on the move by transforming wind energy into electricity and storing it directly to the battery. At the same time, when the sun is out during the day, the car can be charged through the solar panels located on its roof and others portion of vehicles. With this technology, the car can simply run without using electric power from the battery. As long as the solar panels are perfectly working on a sunny day, it is sufficient to charge the battery as well as keep the car running at limited speed. Such complementarities, effectively used of the green resources, but also increases the charge in a storage battery, in order to make up for the inadequacy of pure electric vehicles.

1.2 Research Objectives

After going through the literature review, we came to know that charging the battery of a vehicle by using wind energy and solar energy is the important factor in case of car in a motion. The base car design is a plug-in electric vehicle. The proposed vehicle design is a plug-in hybrid electric vehicle (PHEV) with a solar power system and a wind power system. In this hybrid vehicle design, can use one small scale horizontal axis wind turbine to convert the wind energy into electricity when the vehicle is motion. The wind turbines will be placed on the front of the vehicle. Uses a solar panel to convert directly the solar energy into electricity. At the bad weather condition solar and wind turbine system are not work properly. So, at that time this proposed hybrid electric vehicle's battery charged by a grid connection energy system.

1.3 Scope and Limitations

As fossils fuel resources is decreasing rapidly, we must find alternative solution of this energy crisis and the major solution is using renewable energy likes solar energy, wind energy, geothermal energy, biomass from plant etc. But only solar energy and wind energy are the two promising energy sources for using vehicle.

Solar energy can be captured by solar panels to produce electricity, but this energy is insufficient to move a pure electric car a certain distance. Using this electric energy will increase an electric car's mileage by a few miles per day. The most difficult task in a wind energy system is designing the wind turbine, and installing it up front of the vehicle is also difficult task. Small wind turbine systems are significantly heavier, which has a negative effect on the vehicle's overall efficiency. For this reason, it is important to a light weight material is used for the wind turbine design with more energy capacity properties and long-life cycle.

1.4 Thesis Structure

Chapter 1: The overview of the use of solar energy systems, wind energy systems, and solar and wind hybrid energy systems in electric vehicles are covered in this chapter.

This chapter also covers the significance of renewable energy in the development of environmentally friendly electric vehicles. Details of research object and some future scop, limitation of used solar and wind energy on electric vehicle are also include at this part.

Chapter 2: In second chapter detailly review the solar energy, wind energy and solar and wind power mounted hybrid electric system used in vehicle. This chapter makes it clear which kinds of solar cells and wind turbines are suitable for use in the construction of electric vehicles. Form the journal paper review it is find that which type of material is suitable for design solar and wind hybrid system and also what is the most appropriate position of the installed the wind turbine and solar panel on the vehicle.

Chapter 3: The objectives and aims of your study should be met by your research by employing the best and most useful techniques, the term "research methodology" refers to this. So, in this chapter detailly discuss about the methodology for solar energy conversion system, wind turbine energy producing methodology, solar, wind and plug-in hybrid electric vehicle working methodology. Also, solar and wind energy resource assessment are included in this part of the thesis.

Chapter 4: In this part of the thesis discusses about the availability of solar and wind energy of the location are analysis. In this part find out how much solar energy is currently available at the solar panel area each day and the amount of wind that can be directed attract at a wind turbine blade when a car is moving at a certain speed. Also, it is found that when will get maximum and minimum solar and wind energy.

Chapter 5: In this chapter discusses about the horizontal axis wind turbine blade design, wind turbine design, solar panel design using mono-crystalline silicon solar cell, how to calculation the energy output from the solar and wind energy system. Also discuss about what is the best position to installed the horizontal axis wind turbine and solar panel.

Chapter 6: In this chapter discuss about how these energy outputs depend on certain factors likes weather condition, atmospheric temperature, day and night time etc.

Chapter 7: In this chapter all analysis and simulation results are discuss. From this analysis it is found that how much solar electrical energy and wind electrical energy get from this designed system. Ansys Workbench 2022R and 2016 version are used for wind turbine analysis and solar panel analysis. Efficiency of solar panel and power coefficient of wind turbine and designed hybrid vehicle performance are discussed in this part of thesis.

Chapter 8: This chapter summarizes all the research results, including the performance and efficiency of the vehicle as well as the efficiency of the solar and wind energy systems. The challenges and limitations that came up in the analysis of solar and wind hybrid systems were also covered in this chapter. Finally, make a recommendation for the direction of upcoming research on the vehicle-mounted solar and wind power systems.

Chapter 2

Literature Review

A literature review is an overview of the earlier written works on a subject. The phrase can be used to refer to a whole academic paper or a specific section of a larger academic work, like a book or an article. In either case, the goal of a literature review is to provide the researcher or author and the audience with a comprehensive overview of the body of existing knowledge on the topic at hand. A comprehensive review of the available literature can verify the appropriateness of a research question, theoretical framework, and research methodology. A literature review specifically helps the reader understand the current study's context and place it within the body of the relevant literature. In this sense, a literature review is a scholarly essay that summarises the most recent research on a particular topic, including both substantive findings and theoretical and methodological contributions.

2.1 Solar Energy in Transportation

M. Premkumar and others have done a design, analysis and fabrication of solar PV powered BLDC hub motor driven electric car. The hybrid design system for an EV is proposed, including solar PV, super capacitor, electronic speed controller and storage battery, with the system configuration and different control strategy. In this paper, the vehicles involving battery powered and the charged by PV panels is used for agricultural activities in remote hilly areas. Three 250 W solar panels is used to charging the batteries and the total weight of designed car is nearly 250 kg including the weight of driver. The maximum speed of the car is limited 40 km/h. The vehicles can achieve a maximum speed of 45 km/h for a distance of 100 km, depending on energy saving. [1]

A. Singh and others have done a design of a solar-powered EV charging station for an Indian context and PVsyst 7.2 software has been used for the system design. In this paper the analysis, based on the number of cars charged annually, the monthly variation in energy generation and decreasing in the CO₂ emission using different module

technologies for six Indian cities (Jaisalmer, Ladakh, Delhi, Tawang, Chennai and Bengaluru), has been deliberated. Two modules from 'AEG Solar' (a monocrystalline and a polycrystalline) of 325 Wp and 72 cells are selected and compared for the design. From the solar charging station, the power generated and provided by the 8.1 kWp in each city and different for each month. The power generation varies depending on the climatic factors. Out of the two modules, monocrystalline PV array panels have higher energy generation due to their better efficiency than the monocrystalline PV modules. The charging station generated maximum energy from May to July month. [2]

G.R. Chandra Mouli, P. Bauer and M. Zeman have done a creating an electrical vehicles charging infrastructure using PV panels. The system is designed for the use in workplaces in Netherlands to charge electric cars of the employees as they are parking during the day time. In this paper, two scenarios are considered- one where the electric vehicles have to be charged only on weekdays and another one EV have to be charged per day. In this paper, a 10 kW EV-PV charger will be using for the charging and discharging of a vehicle up to 10 kW. The solar power is generated by using a 10 kWp PV array that could be located on the roof top of the buildings. They assumed the efficiency of the charging/discharging of the battery including power exchange is 93% and the efficiency of power conversion with the grid is considered as 95%. In the Netherlands, the power converter can be undersized with respect to the PV array by 30%, and resulting in a loss of only 3.2%. From the designed they can get 30 kWh energy to the EV for both 5 days/week and 7 days/week EV load and resulted in minimum energy exchange with the grid. [3]

P. Shankar Sahu and others have done on design the mini car with environmentally friendly materials and power by solar energy. This paper explains how the solar energy produced by the solar radiation able to generated electricity by using multi crystalline solar panel. In this paper, various significant factors like maximum allowable speed during a turn, gyroscopic forces, position of centre of mass and etc are determine using the physical test. From the analysis of load vs velocity graph, they conclude that the solar car model has load bearing capacity higher than its own load and initially the velocity moderately decreases with increase in load. They can find the load carrying efficiency is 71.81% and the mechanical efficiency is 93.34% of the design car. [4]

S. Maitreya, H. Singh Dangi, N. Singh Naruka and P. Paliwal research on the solar power electric vehicle. In this paper, aims to present the improvement in range that can be brought about by using solar photo-voltaic (PV) modules on an EV. They used MATLAB for the simulation. The simulation involved exposing the PV module to sunlight continuously for a period of 5 hours and allowing the energy produced by it to be stored by the battery via a DC-DC converter. From the PV solar panel, they generate 245.05089 Wh power and stored in a Lithium Magnesium Iron Phosphate (LMFP) battery via a DC-DC converter with feedback. [5]

S. Manivannan and E. Kaleeswaran suggested developing an electric vehicle with a mounted polycrystalline solar panel system. The project's objective is to advance solar panel technology that encourages the use of green energy; picture a scenario in which solar power could be used to recharge electric cars, which would also have solar panels integrated into the vehicle. How useful would this be in a rainy climate is the next query. This proposed electric vehicles already have many of their features likes security system, navigation system, route detection, Wi-Fi, Battery Update, and LoRa support are all included. The solar panels built into the vehicle can generate 500 W of power when the sun is directly overhead. This proposed system a 24 V 25 Ah lead-acid battery are used for low cost and the total capacity of the battery system will be 600 Wh to run for 6 hours of the proposed vehicle. A Brushless DC motor (BLDC) is used with greater than 75% efficiency and higher life time compared to Brushed DC motors. The SPEV dimension is 200cm×120cm×160cm and seating capacity of single person. From the analysis results, the total power consumption by vehicle for 6 hours per day is 2460 Wh and the total energy generated by proposed solar panel is 2500 Wh. [6]

W.K. Alani and others working on enhancing the fuel consumption saving and emission reduction on light-duty vehicle by a new design of air conditioning working by solar energy power system. Normally air conditioning system of a vehicle (AC) increases the fuel consumption about 20% of total energy produce by the engines due to extra load needs for ac operation. An innovative solar-powered air conditioning system was used to satisfy the study's energy requirements and improve the fuel efficiency of vehicles. The air conditioning system was connected to a flexible photovoltaic cell (PV) in order to counteract the electricity produced by the vehicle engine. Both cooling and heating scenarios put the saloon car's air conditioning system to the test. It was found that the solar-

powered air conditioning system consume 25% less engine fuel compared to a typical air conditioning system. According to the results of the air conditioning system, on a hot day, the cooling temperature inside the car drops to 20°C in less than a minute while the outside temperature is 40°C. From the analysis It was found that a solar air conditioning system outperforms a traditional air conditioning system in terms of BSFC and emissions reduction, engine performance improvement, and energy efficiency. [7]

M. Awad and others designed and analysis of a photovoltaic (PV) system to charge five models of electric vehicle (EVs) such as BMW i3 2019, Volkswagen e-Golf, Fiat 500e, Mercedes EQA 250 and Hyundai Kona Electric in a DC fast charging mode by using a DC-DC buck converter for the maximum output and efficiency from PVs are obtained. In this proposed used a Perturb and Observe (P&O) Maximum Power Point Tracking (MPPT) charging converter. The MATLAB program is used to simulate the EV models by calculating the MPPT controller's efficiency, the charging time, and the characteristics of the voltage and current levels for each model of these EVs. All analysis done under the condition of solar irradiance level from 600-1000 W/m² and temperature between 20-30°C. PV modules are designed in system with 1500 V and different ranges of Li-ion battery. Crystalline silicon wafer-based cells are used in the modules. A PV array is a collection of strings that are connected in parallel. Strings are used to connect some of the PV modules in series. From the analysis result, the time of the charge for five types of electric vehicles is near its range according to the electric vehicles database. [8]

Z. Jin, D. Hao and others designed and analysis a portable auxiliary photovoltaic power system for electric vehicle based on a foldable scissors mechanism for electric vehicle. A photovoltaic power generation module that can be folded up to five times smaller than it is when it is unfolded was developed using a foldable scissors mechanism. The energy efficiency of the PV system in EVs is modelled and evaluated using a Simulink model in MATLAB using variables for solar irradiance and ambient temperature. This model can be used to calculate the power output of any mobile photovoltaic system, allowing for the optimization of both the energy efficiency and PV size. The designed system consists of two main parts: a PVPGM and an electricity transfer module. Maximum output powers of 1.736 W and maximum electricity transfer efficiencies of 57.7% are obtained by the solar simulation experiment with loads of 5 and 10, respectively. The annual electricity generated by proposed fordable PV system is 2.033

GWh. The proposed photovoltaic power generation module has a surface area of only 0.47 m^2 , while a car typically takes up more than 10 m^2 . As a result, it is possible to expand the photovoltaic power generation module's surface area and boost its output power for electric vehicles. [9]

Y. Ota, K. Araki and others designed a standard group of curved surfaces to statically analysed the roof shapes of commercial vehicle and calculate the PV coverage for various surface. In this study, the distributions of roof sizes and shapes used in this study came from trace drawings of various passenger cars. Using Monte Carlo simulations and commercial vehicle statistics, produced a set of curved surfaces as described in this analysis. Following that, this was used to compute the distributions of the mechanical and optical properties. On the basis of the results, broad recommendations were made, one of which was a 96% potential coverage ratio for a hemispherical roof with a 1000 mm radius of curvature. [10]

2.2 Wind Energy in Transportation

Peter W. Ripley conducted research in designing a system for harnessing the wind energy to charge the battery of a vehicle. In this design used two wind turbine one is internal wind turbine another is external wind turbine. When a vehicle is motion then the internal wind turbine is invented to create electric current charge to vehicles batteries. External wind turbine is invented to provide current charge to batteries while the vehicle is parked. The internal wind turbine that mounts to the roof of the vehicle after a vertical-directed, through hole has been created in a central portion of the roof and external wind turbine also mounts to roof of the vehicles. [11]

Kajal A. Gulhane targeted to research the design and implementation of a vehicle wind turbine, that can be attached in electric cars to generate electric power to charge the car batteries when car in motion. In this paper, a portable horizontal axis diffuser augmented wind turbine is adopted for the design as it is able to produce higher power output when compared to the conventional bare wind turbines. Based on the research, when the car is moving at a speed of 120 km/h, a significant amount of electric power 3.26 kW is restored to the batteries. [12]

Souad A. M. AlBat'hi, M Hazaw Haszard and others researched to find a light weight material which is suitable for wind turbine blade. In this paper, rice straw fibre was used as a reinforced agent in composite with polypropylene as matrix and the composite was then characterized by mechanical testing for tensile, flexural and impact as well as density measurement, Scanning Electron Microscopy (SEM) and Dynamic Mechanical Testing (DMA). From this experiment, it is found that the mechanical properties of composite are improved with increases of rice straw content and also found that the use of MAPP as coupling agent is able to improve the bonding between polypropylene matrix and rice straw fibre. This composite material can be an alternative material for small scale horizontal axis wind turbine blade. The materials with nanoengineered matrix and microscale reinforcement can show up to 80% higher fracture toughness and lifetime of blades materials. [13]

Feng-Tsai Weng, Yao-Xian Huang are together investigating the energy-saving efficiency of a car, a horizontal-axis wind turbine of 400 W was mounted to the front bumper of the car. They use two types of wind turbine arrangement for charging the vehicle battery. One is an electromagnetic clutch was designed for cutting charge system by wind turbine with a button in the car. And another one is the generator which is driven by engine pulley system when vehicle starts, it can be switched driven by wind turbine while the vehicle moves at a stable speed on road. In this paper, charge efficiency of the wind turbine was compared, and fuel also investigated fuel consumption when different length of wind turbine blades was used at different car speed. From this paper, we can say proposed wind turbine system reduced the fuel consumption about 15% in a 30 km distance. The result of the experiments shows that blade length 40 cm have better charging efficiency. The charging efficiency is increased to higher speed of the vehicle. [14]

E. El, C. ildiz, B. Dandil and A. Yildiz have designed an electric vehicle with wind energy raised by on-the-go vehicles and thus enhancing the distance covered at one single charge. In this paper, they research on effect of wind turbine designed for electric vehicles on aerodynamics and energy performance of the vehicle. They are using the shear stress transport $k-\omega$ turbulence model, CFD simulations for to determine the drag coefficients, pressure contours and velocity vectors of the designed basic vehicle model (M_0) and its two different modified versions (M_1, M_2). M_0 is a base designed vehicle and M_2 is the vehicle designed with wind horizontal axis wind turbine system. The ANSYS software was used for the numerical simulations. That model vehicle had an

overall length of 4625 mm, a width of 1730 mm, and a height of 1482 mm. The analyses have been performed at a speed of 27 m/s for each vehicle model of the designed modification. The maximum pressure occurred in the front bumper area of the vehicle for all three model. The M_0 model had the lowest drag coefficient value. From the simulation result they found, the total energy loss of the M_2 model increased by 2.47% compared to the M_0 model but the overall energy gain approximately 5.13% of the total energy loss of M_0 model. [15]

G. R. Kalagia, R. Patila and N. Nayak together experimental study on mechanical properties of natural fibre reinforced polymer composite materials for wind turbine blades. In this study, wind turbines are constructed using composites made of natural fibre reinforced polymers. Examination will be done of the specifications for the composites, as well as their traits, parts, production methods, manufacturing technology and defects. There will also be discussion of promising future directions for their development. These benefits of natural fibre-reinforced polymer (NFRP), including low cost, low density, non-abrasive qualities, biodegradability, and renewable nature, cannot be attained by synthetic fibre-reinforced composites. Wind turbine parts are constructed from unattractive environmental materials. After a large structure has served its purpose, which for modern wind turbines is estimated to be 20 years, it will eventually need to be disposed of to the environment. As a result of this ongoing focus, scientists and engineers are working to replace the current material system of wind turbines with biodegradable materials. Natural fibre reinforced composites, one of these classes of materials, have superior mechanical properties as well as being naturally biodegradable. [16]

Z. Belfkira, H. Mounir and A. EL Marjani working on optimize the materials of wind turbine blades using natural fibre through a hybridization technique. In this innovative concept, kenaf fibres are mixed into a hybrid composite material that was originally made of synthetic fibres. To maintain the best possible aerodynamic performance while optimizing the aerodynamic shape of the wind turbine blade, a thorough analysis was first conducted. Second, ANSYS Computational Fluid Dynamics (CFD) was used to calculate the aerodynamic parameters needed later in the structural justification. When the blade geometry was finally imported into PATRAN software, a comprehensive analysis of the blade structure was established, taking into consideration the new combination of the three

types of fibres: carbon, glass, and kenaf fibres. An analysis based on material resistance, weight, and cost savings in comparison to the non-optimized model showed a weight saving of 40%, a material cost saving of 67%, and a tip deflection of roughly 17% less than the allowed threshold. [17]

A. Gupta and N. Kumar are modelling a car was used to model two ducts with various cross sections and a fan connected to an alternator. Simultaneously, simulations were carried out in Ansys Fluent for wind speed and torque analysis for alternator power calculations. In this analysis, torque was calculate using fan model in the Qblade software with NACA 5510 aerofoil at a vehicle speed range 121-147 m/s. The fan model consists of five 110 mm long blades with 20 mm hub radius. This fan was optimized to run at incredibly low TSR range of 0.15 to 0.3 in order to produce the desired amount of torque. Experimental studies were conducted on the alternator modification to convert the low voltage DC output into high voltage AC output to power the vehicle batteries. The range of rotational speed for the fan was 1500 to 2000 RPM. For the power requirements of the alternator, the torque generated will be in the range of 25 to 30 Nm. The results show that an increase in the overall range of electric vehicles of about 23% would make them sustainable. [18]

A.M. Abdelsalam and others study numerically the effect of curvature of linear blade profile on the performance of small-scale horizontal axis wind turbine. In this paper, investigated are rotors with two types of curvature: forward angles of 5, 10, 15, 20, 30, and 45 degrees; and backward angles of -5, -10, and -15 degrees. Additionally, three $r/R = 0.8, 0.9, \text{ and } 0.95$ curvature positions are studied. In this analysis used both the Reynolds-averaged Navier-Stokes (RANS) equations and the Shear Stress Transport (SST) k-turbulence model CFD simulation. The airfoil used S809 with rotor radius of 5.026 m. In comparison to the other rotors, it is found that the one with $r/R=0.9$ and a forward curvature of 5 degrees has the highest power coefficient. The proposed rotor reduces axial thrust by about 12.5% when it is operating at its highest efficiency and increase the power coefficient by amount 2.18%. For the tip speed ratios of 5 and 6, which are responsible for the performance peak, the separation in this case almost completely disappeared. [19]

2.3 Integration of Solar and Wind Energy in Vehicle

K. Someswara Rao and others have done on design and analysis of an autonomous hybrid vehicle and the hybrid vehicles used three different ways of renewable energy sources that are solar energy, wind energy and fuel cell technology to generate electricity for running the vehicle. Various sensors are used in this design for autonomous vehicles. Sensors are IR sensors, temperature sensor, radar receivers, humidity sensor at the front side of the car and parking sensor, parking camera, obstacle sensor, rear collision sensor etc. The design car is successful tested under a load of 30 kN and a velocity of 30 m/s. [20]

D. Limenew Meheretie and Keadsew Wall [2015] designed a charging and controlling circuit of electrically operated auto rickshaw for the public utilities. They put a wind turbine and solar panel at the top of the auto rickshaw. They used three 1m by 1m solar panel at the top and the back side of the vehicle. They can generate 1050 W power from the three 1m by 1m solar panels by nine sun shine hour per day. Design car can be driven for 4 hours using solar panels. From wind turbine they can generate power 650 Wh and using only wind turbine they can operated the car hours 30 minutes. From the simulation results we can say that the design is sufficient to derive the car.

A. Tekle study on renewable energy use, by integrating solar and wind energy for continuous electric car battery charging capacity in mobility and battery charging potential was performed using MATLAB. This design vehicle can charge using wind and solar during motion and plug-in and solar energy can also during immobility with parallel confirmation. In this vehicle designed two 50 cm diameter horizontal axis wind turbine are installed at the front and one vertical axis wind turbine is installed at the top on the vehicle and obtain up to 2.5 kW rated power at rated speed of the turbine around 25 m/s. In this paper uses 6 photovoltaic module and these modules contain 36 series PV cells and total area cover by PV arrays reaches 2.16 m^2 with 100 cm^2 area of each PV cell. The power get from the design PV cells varies from 400-800 W. [21]

T. Vignesh, S. Sathishkuma, D. Silambarasan together discusses about the usage of solar energy and wind energy to power up the vehicle. The electrical charge is consolidated from the photovoltaic panel and wind turbine and directed to the output

terminals to produce low voltage (Direct Current). In the paper, the characteristic features of the components: PV solar panel, wind turbine, charge controller, battery, interleaved converter, Arduino processor and BLDC motor required for the vehicle application were studied in real time and also were modelled individually and the complete hardware integration of the system into meet up the application's requirement. For solar energy conversion they used 36 multi-crystallin PV cells and the rated output power is 140 Wp. For the wind energy conversion, they used a horizontal-axis wind turbine (HAWT). Based on the simulation results and analysis, it could be concluded that the proposed hybrid system can be satisfactorily used in the Pehentian Islands. [22]

Md. Arman Arefin and A. Mallik, research on using both wind and solar energy system in engine driven auto-rickshaw along with a plugged-in hybrid technology. In this paper, a model of the vehicle is proposed for the placement of the turbine inside the vehicle and the model is validated by ANSYS CFX simulation. A novel CFD simulation is conducted for wind turbine blade considering reasonable data. In this designed two solar panel that contain 60 mono-crystalline cells and a horizontal axis wind turbine placed inside the vehicle. The efficiency of solar panel is approximately 18% and total rated output is 12V-180 kW. The efficiency of wind turbine is 60.35% and mechanical output is 2 HP. In fine, the proposed vehicle is more synchronized than conventional vehicles and the proposed methodology can be implemented in different other vehicles. [23]

T. Jayaraj, R. Joy and others proposes a hybrid electric vehicle (HEV) system. The hybrid electric vehicle design is made using wind energy and solar energy system. To covert solar energy to electrical energy solar panel is used and its converts approximately 30 to 40% of solar radiation into electric energy. They used maximum power point technology (MPPT) to get maximum power from the solar panel. DC shunt generators are used in windmills to switch mechanical to electrical energy also avoids the usage of inverter. the SEPIC, operating as a DC-DC buck-boost converter is used so that it can bring the output in a specified level to control the duty ratio, incremental conductance (INC) based maximum power point tracking (MPPT) is utilized. The performance of the proposed system is analysed using MATLAB/SIMULINK platform. This proposed system obtained output is 15 V, it will derive a DC motor. Based on the

simulation results and analysis, it can conclude that the proposed hybrid electric system can be satisfactorily used in the hybrid electric vehicle. [24]

W.A. Eltayeb and others designed and analysis a hybrid tree is an artificial structure resembling a natural tree with branches on top of which are mounted solar modules or wind turbines. In this paper using a two-axis tracking system, the 3-kW hybrid tree design presented, which will be put in place at Vaddeswaram, Andhra Pradesh (16.26 N, 80.36 E), can produce the most energy. It will be made up of 1 kW of wind power and 2 kW of solar power. In this paper MATLAB software used for analysis and simulation. The maximum value of C_p is 0.48 is achieved at pitch angle $\beta = 0$ and $\lambda = 8.1$ and considered as nominal value. The proposed solar-wind hybrid tree can produce 3763 kWh/year instead of 4709 kWh/year with the two-axis tracking system if solar panels are fixed at an 18.25 tilt angle. [25]

Chapter 3

Methodology

The research methodology is a structured approach that helps select the most effective methods for this study, aligning with its purpose and objectives. In this context, a hybrid system is introduced, combining plug-in charging technology with a PV solar panel and a wind turbine. The solar panel converts solar energy into electricity, while a horizontal-axis wind turbine transforms wind.

3.1 System Architecture and Design

In order to power this hybrid plug-in electric car, monocrystalline silicon solar cells and a horizontally oriented wind turbine were used. The solar panel is mounted on the roof, and the wind turbine is mounted in front of the car. Due to aerodynamic pressure, the wind turbine rotates when the car is moving and generates electricity by using a low-speed permanent magnet DC generator or Dynamo. During the day, rooftop solar panels converted solar energy directly into electrical energy.

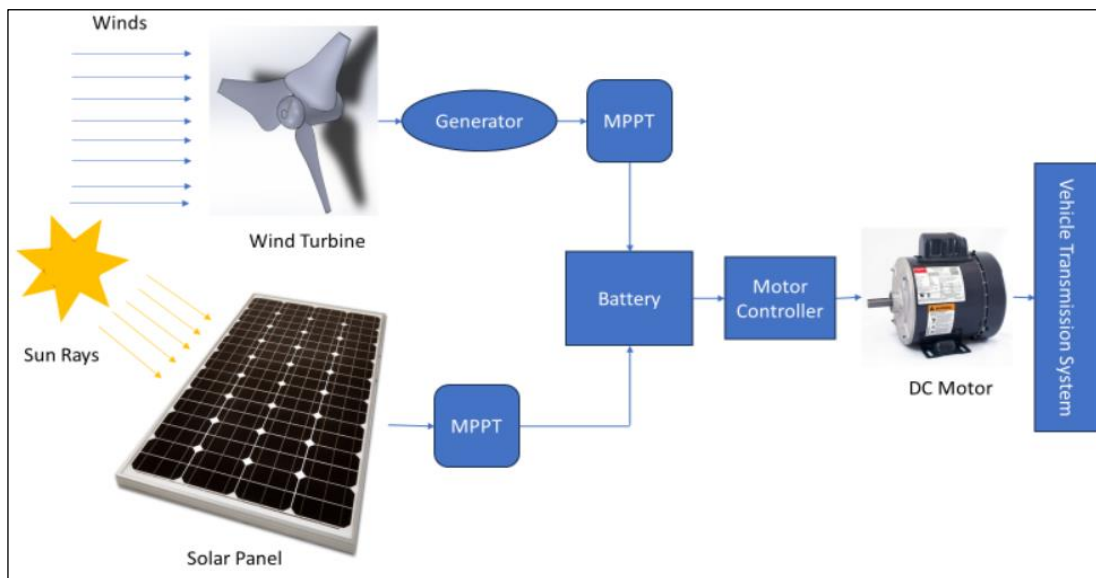


Fig. 1: Schematic diagram of Solar and Wind Power System

3.2 Solar Energy Integration

In this propose system, the PERC mono-crystalline silicon photovoltaic cells are used to convert solar power into electric energy. The photovoltaic panels of solar power generation system can generate electrons and holes under the condition of light, so as to generate an electric current. ANSYS software use for simulation and power calculation of the photovoltaic system. The global formula to estimate the electricity generated in output of photovoltaic system is:

$$E_s = A_s \times \eta_s \times H \times PR$$

Where,

E_s = Energy (kWh)

A_s = Total solar panel area

η_s = Solar panel yield or efficiency (%)

H = Annual average solar radiation on tilted panels (shadings not included)

PR = Performance ratio, coefficient for losses (range between 0.5 and 0.9, default value = 0.75)

Solar Cell Efficiency Calculation:

The solar cell efficiency calculation formula is, $\eta_s = 0.28 - 0.001(T_{cell})$ [26] [27] [28]

Where, T_{cell} is the average temperature of solar cell.

3.3 Wind Energy Integration

In this proposed system, a horizontal-axis wind turbine in the front of the vehicle has been used. Wind generator mainly consists of the blade of wind turbine generators rectifier and controller. The torque of wind overcome the engine's internal resistance to produce kinetic energy, then converted it into electrical energy.

The amount of power obtained from the wind of velocity is given by the equation,

$$P_w = \frac{KE}{t} = 0.5 \times \rho \times A_w \times V^3$$

P_w is the available theoretical wind mechanical power in watts.

Actual power output from the wind turbine,

$$P = \frac{1}{2} \rho A_w C_p(\lambda, \beta) v^3$$

Where, C_p is the power coefficient of wind turbine and this is function of γ and β .

λ is the fan blade tip efficiency of bearing speed ratio.

β is the pitch angle.

C_p can be determined by the following formula:

$$C_p(\lambda, \beta) = c_1 \left(\frac{c_2}{\lambda_i} - c_3 \beta - c_4 \right) e^{\frac{-c_5}{\lambda_i}} + c_6 \lambda \quad [29]$$

The λ_i satisfy the following formula,

$$\frac{1}{\lambda_i} = \frac{1}{\lambda + b_0 \beta} + \frac{b_1}{\beta^3 + 1}$$

Where, $c_1, c_2, c_3, c_4, c_5, c_6, b_0, b_1$ are all the constant that determined by the fan manufacturer.

The amount of mechanical power obtained from the wind of velocity is given by the equation,

$$P_w = \frac{1}{2} \rho A C_p(\gamma, \beta) v^3 N_g N_b$$

Where, N_g is defined as the efficiency of gearbox.

N_b is the efficiency of bearings.

After getting mechanical power, used a DC WTGs generator for convert this power into electric power. The equation of this conversion,

$$P_e = \eta_g P_w$$

Where, P_e is electric power that can be obtained from the WTGs.

η_g is the efficiency of the generator.

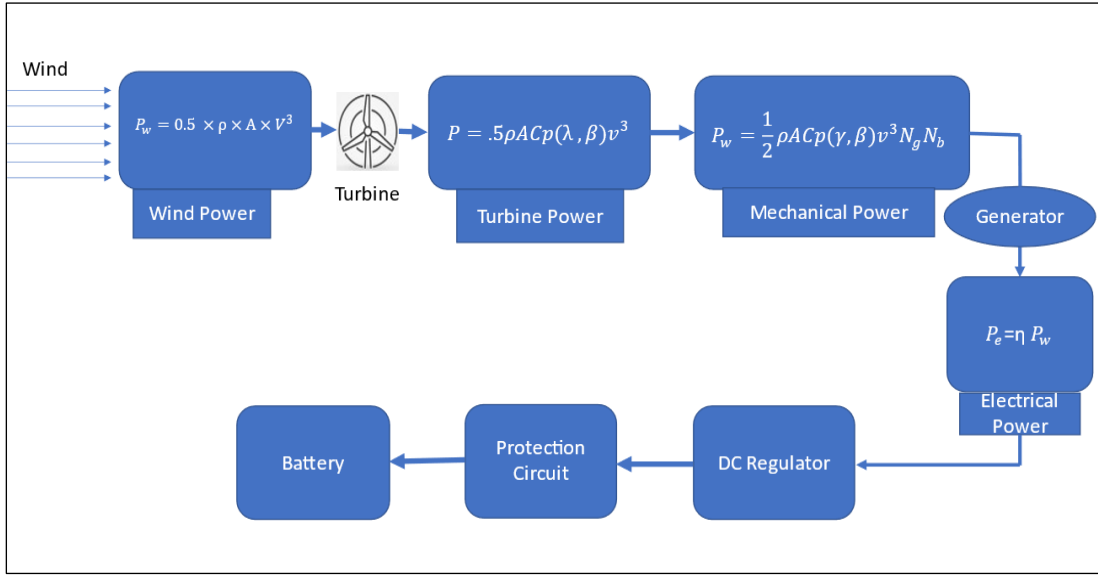


Fig. 2: Schematic diagram of Wind Turbine Power Conversion

After receiving electric power from generator, a protection control system will be used to store it in the vehicle battery.

3.4 Testing and Validation

The global formula to estimate the electricity energy generated of photovoltaic system is:

$$E_{theoretical} = A_s \times \eta_s \times H \times PR$$

$$E_{theoretical} = 2.64 \times 0.215 \times 976.12 \times 0.75$$

$$E_{theoretical} = 415.53 \text{ Watts}$$

Now, from simulation the output energy from the same design solar panel is 391.43 Watts. In this analysis percentage of error is,

$$= \frac{(415.53 - 391.43)}{415.53} = 5.7 \%$$

Actual theoretical power output from the wind turbine at 60 km/h relative wind speed,

$$P_{theoretical} = \frac{1}{2} \rho A_w C_p(\lambda, \beta) v^3$$

$$P_{theoretical} = \frac{1}{2} \times 1.22 \times 0.204 \times 0.26 \times 16.67^3$$

$$P_{theoretical} = 149.87 \text{ Wh}$$

From the analysis and simulation of horizontal wind turbine at 60 km/h relative wind speeds the output electric power is 150 Wh at 25° of AOA. In this analysis percentage of error is,

$$= \frac{(150 - 149.87)}{149.87} = 0.1\%$$

Table 1: Validation report of Solar and Wind Power System

Energy System	Theoretical Power	Analytical Power	% Error
Solar Panel	415.53	391.43	5.7
Wind Turbine	150	150	0.1

Chapter 4

Solar and Wind Energy Resource Assessment

4.1 Solar Energy Resource Assessment

Solar energy comes from the sun and can be turned into electricity or heat. It's the cleanest and most abundant form of renewable energy. Solar panels help capture this energy, which can be used for making electricity, providing light, ensuring cozy indoor environments, and supporting business and industry needs.

Solar Forecasting: [30]

Solar power forecasting is the process of gathering and analysing data in order to predict solar power generation on various time horizons with the goal to mitigate the impact of solar intermittency. Solar power forecasts are used for efficient management of the electric grid and for power trading.

Solar power forecasts rely on factors like the sun's position, sun's path, weather conditions, light scattering, and solar plant features. The accuracy of these forecasts varies with the prediction timeframe.

i. Nowcasting (forecasting 3-4 hours ahead): Solar power nowcasting predicts solar energy production for the next few minutes to a couple of hours with high accuracy, often up to 90%. These forecasts typically provide updates every 5 to 15 minutes, sometimes even every minute. The actual nowcast is then frequently enhanced by e.g., Statistical techniques. In the case of nowcasting, these techniques are usually based on time series processing of measurement data, including meteorological observations and power output measurements from a solar power facility. What then follows is the creation of a training dataset to tune the parameters of a model, before evaluation of model performance against a separate testing dataset. This class of techniques includes the use of any kind of statistical approach, such as autoregressive moving averages (ARMA, ARIMA, etc.), as well as machine learning techniques such as neural networks, support vector machines, etc.

ii. Short-term forecasting (up to seven days ahead): Short-term forecasting gives us forecasts for up to a week ahead. These accurate forecasts rely on various data sources like weather data, local conditions, and ground observations, combined with complex math models.

Ground based sky observations:

For intra-day forecasts, local cloud information is acquired by one or several ground-based sky imagers at high frequency (1 minute or less). The combination of these images and local weather measurement information are processed to simulate cloud motion vectors and optical depth to obtain forecasts up to 30 minutes ahead.

Satellite based methods:

These methods leverage the several geostationary Earth observing weather satellites (such as Meteosat Second Generation (MSG) fleet) to detect, characterise, track and predict the future locations of cloud cover. These satellites make it possible to generate solar power forecasts over broad regions through the application of image processing and forecasting algorithms. Some satellite-based forecasting algorithms include cloud motion vectors (CMVs) or streamline based approaches.

Numerical weather prediction:

Most of the short-term forecast approaches use numerical weather prediction models (NWP) that provide an important estimation of the development of weather variables. The models used included the Global Forecast System (GFS) or data provided by the European Centre for Medium Range Weather Forecasting (ECMWF). These two models are considered the state of the art of global forecast models, which provide meteorological forecasts all over the world.

In this curve below, the variation of solar radiation energy with respect to a particular day (18th June to 21st June in 2023) with 15 minutes interval can be seen. From this curve it is evident that the daily global irradiance is 13.1 KWh/m² and the maximum solar irradiance at 1 PM is 1008 W/m². Also, from this curve the temperature variation of that day can be seen. The maximum temperature of that day was 40°C at 1 PM.

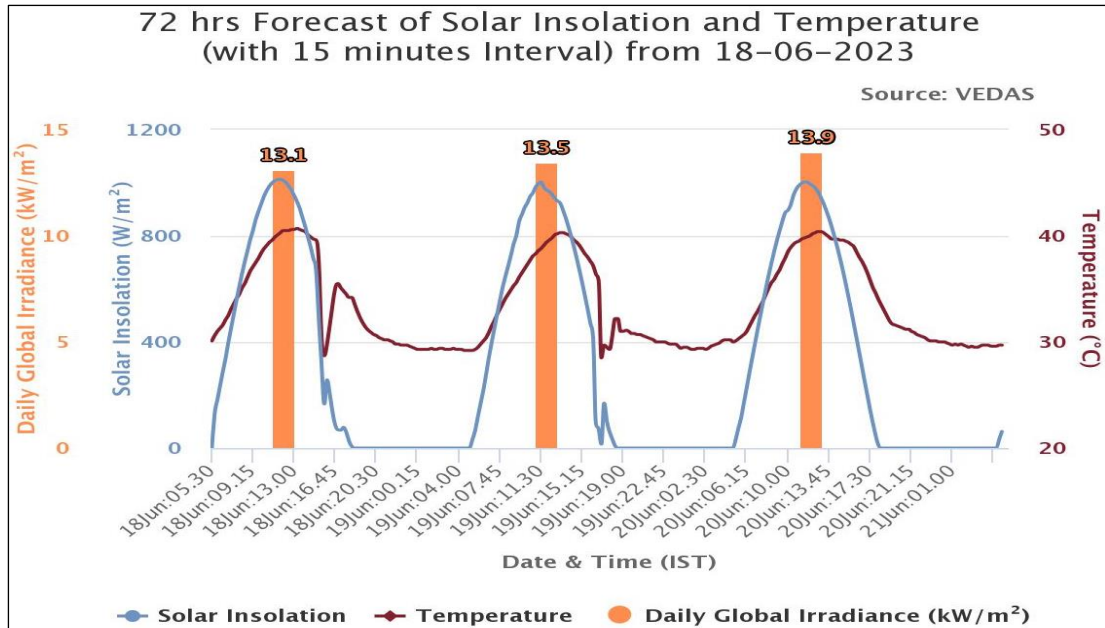


Fig. 3: Graph plot of Daily Global Irradiance and Temperature with 15 minutes interval from 18-21 July, 2023

iii. Long-term forecasting (weeks, months, years): *Long-term* forecasting usually refers to forecasting techniques applied to time horizons on the order of weeks to years. These time horizons can be relevant for energy producers to negotiate contracts with financial entities or utilities that distribute the generated energy. In general, these long-term forecasting horizons usually rely on NWP and climatological models. Additionally, most of the forecasting methods are based on mesoscale models fed with reanalysis data as input. Output can also be postprocessed with statistical approaches based on measured data. Due to the fact that this time horizon is less relevant from an operational perspective and much harder to model and validate, only about 5% of solar forecasting publications consider this horizon.

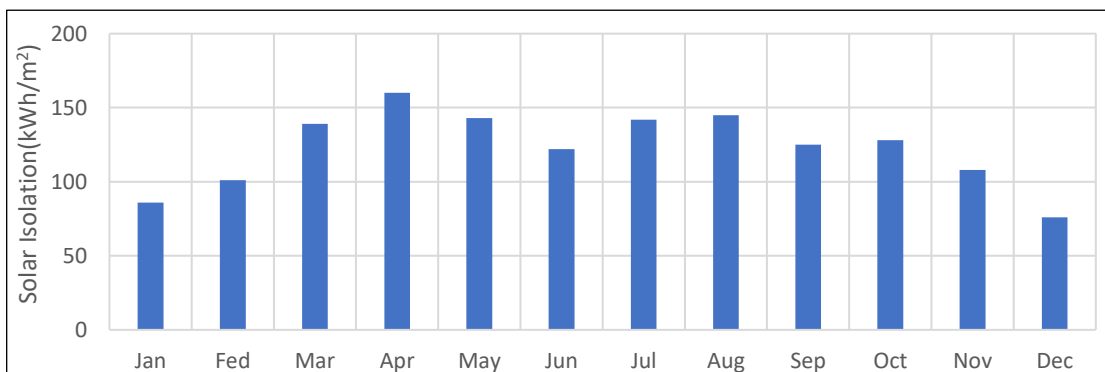


Fig. 4: Graph plot of Solar Insolation (kWh/m²) with months

From this graph, it can be seen that the maximum amount of solar radiation energy (160 kW/m^2 falling in the month of April. The average solar radiation energy falling in per month is 122.9 kW/m^2 . So, the total solar energy falling per meter square is 1475 kW/m^2 .

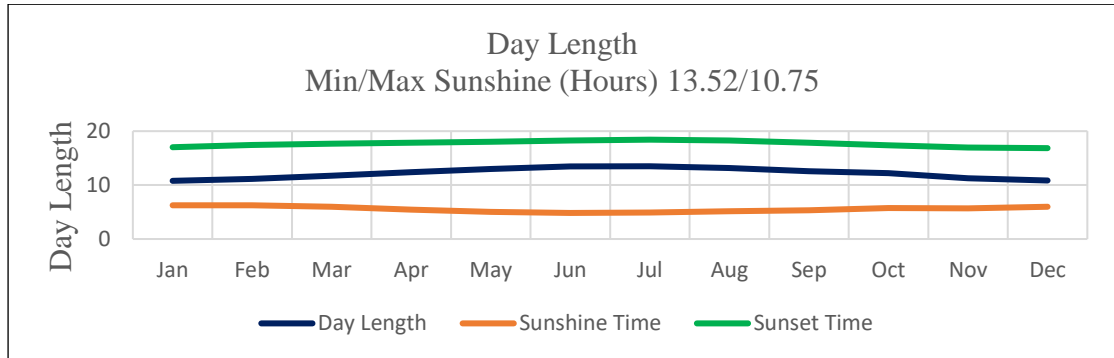


Fig. 5: Graph plot of available Day Length varying with months

Using this graph, the average day length in Kolkata can be found. From the curve, average day length is 10.5 hours per day. This length of day means that the design solar panel will generated electricity efficiently at 10.5 hours per day.

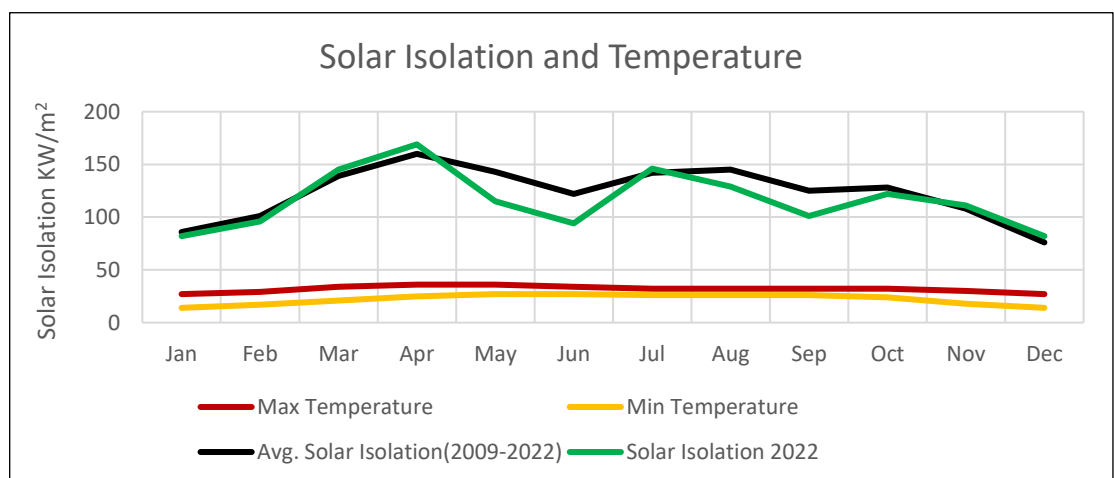


Fig. 6: Graph of 16 years average Solar Insolation and Temperature with respect to months

From this graph we can see that the variation of 15 years average maximum and minimum solar insolation energy in per month. Maximum value of solar radiation energy is 223 kW/m^2 at months of July and minimum value of solar radiation energy is 82 kW/m^2 at month of December.

4.2 Wind Energy Resource Assessment

In this setup, a compact horizontal-axis wind turbine is installed at the front of the vehicle. When the wind flows over the turbine blades, it creates a pressure difference on each side, resulting in both lift and drag forces. The lift force dominates and drives the rotation of the turbine blades.

However, in this design, when the vehicle is moving forward at a specific speed, the wind turbine is being forced by the aerodynamic pressure force. This aerodynamic pressure force is causing a pressure difference on each side of the wind turbine blade. The lift and drag force components are produced as a result of this pressure difference, and they are normal to the blade and its axis, respectively. The potential of the lift force is greater than that of the drag force. This lift force helps the wind turbine blade rotate with respect to its horizontal axis. The analysis identifies the vehicle speed at which the wind turbine is working most effective.

4.3 Hybrid Electric Vehicle

An electric vehicle (EV) relies on one or more electric motors to drive it, and it can draw power from external sources through a collector system or operate independently using a battery that may be charged through various means like solar panels, wind turbines, or fuel cells.

EVs first came into existence in the late 19th century, when electricity was among the preferred methods for motor vehicle propulsion, providing a level of comfort and ease of operation that could not be achieved by the gasoline cars of the time. Internal combustion engines were the dominant propulsion method for cars and trucks for about 100 years, but electric power remained common place in other vehicle types, such as trains and smaller vehicles of all types. In the 21st century, EVs have seen a resurgence due to technological developments, and an increased focus on renewable energy and the potential reduction of transportation's impact on climate change, air pollution, and other environmental issues. Project Drawdown describes electric vehicles as one of the 100 best contemporary solutions for addressing climate change.

Type of Electric Vehicles: It is generally possible to equip any kind of vehicle with an electric power-train.

i. Pure Electric Vehicles: A pure-electric vehicle or all-electric vehicle is powered exclusively through electric motors. The electricity may come from a battery, solar panel, wind turbine or fuel cell.

ii. Hybrid Electric Vehicles (HEVs): A hybrid electric vehicle (HEV) is a type of hybrid vehicle that combines a conventional internal combustion engine (ICE) system with an electric propulsion system (hybrid vehicle drivetrain). The presence of the electric powertrain is intended to achieve either better fuel economy than a conventional vehicle or better performance. The most common form of HEV is the hybrid electric car, although hybrid electric trucks (pickups and tractors), buses, boats and aircraft also exist.

Today's hybrid vehicles (HEVs) incorporate technologies like regenerative brakes, which capture energy when you brake and store it in a battery or supercapacitor. Some HEVs also employ an internal combustion engine to operate an electrical generator, either recharging the batteries or directly driving the electric motors. This setup is referred to as a motor-generator system.

There are different ways that a hybrid electric vehicle can combine the power from an electric motor and the internal combustion engine. The most common type is a parallel hybrid that connects the engine and the electric motor to the wheels through mechanical coupling. In this scenario, the electric motor and the engine can drive the wheels directly. Series hybrids only use the electric motor to drive the wheels and can often be referred to as extended-range electric vehicles (EREVs) or range-extended electric vehicles (REEVs). There are also series-parallel hybrids where the vehicle can be powered by the engine working alone, the electric motor on its own, or by both working together; this is designed so that the engine can run at its optimum range as often as possible.

iii. Plug-in Electric Vehicle (PEVs): A plug-in electric vehicle (PEV) is any motor vehicle that can be recharged from any external source of electricity, such as wall sockets that connects to the power grid, and the electricity stored in the rechargeable

battery packs drives or contributes to drive the wheels. Plug-in electric vehicle is a subset of electric vehicles, and includes all-electric or battery electric vehicles (BEVs) and plug-in hybrid vehicles (PHEVs).

iv. Range Extended Electric Vehicle: A range-extended electric vehicle (REEV) is a vehicle powered by an electric motor and a plug-in battery. An auxiliary combustion engine is used only to supplement battery charging and not as the primary source of power.

v. Fuel Cell Electric Vehicle (FCEV): Fuel Cell Electric Vehicles (FCEVs), also known as fuel cell vehicles (FCVs) or Zero Emission Vehicle, are types of electric cars that employ ‘fuel cell technology’ to generate the electricity required to run the vehicle. In this type of vehicles, the chemical energy of the fuel is converted directly into electric energy.

On-and off-road EVs, Rail borne EVs, Space Rover Vehicles, Airborne EVs, Seaborne EVs, Electrically Powered Spacecraft and etc. are some of the more types of electric vehicle in the market.

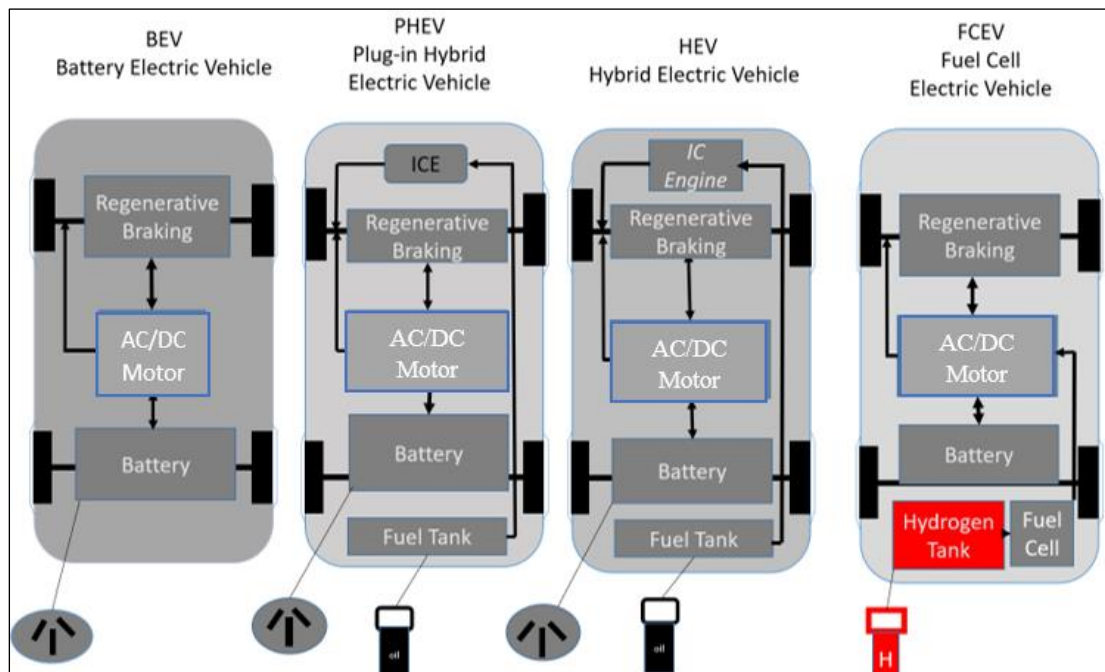


Fig. 7: Schematic diagram of different types of Hybrid Electric Vehicle

Components of Electric Vehicle: Electric vehicles consist of an electric motor that is powered by a battery pack. The main advantage of electric vehicles is that they emit zero emissions and are eco-friendly. They also do not consume any fossil fuels, hence use a sustainable form of energy for powering the car. The main components of electric vehicles are:

DC-DC convertor: The DC-DC convertor distributes the output power that is coming from the battery to a required level. It also provides the voltage required to charge the auxiliary battery.

Traction Battery Pack: Traction battery pack is also known as Electric vehicle battery (EVB). It powers the electric motors of an electric vehicle. The battery acts as an electrical storage system. It stores energy in the form of DC current. The range will be higher with increasing kW of the battery. The life and operation of the battery depends on its design. The lifetime of a traction battery pack is estimated to be 200,000 miles.

Electric Motor: Electric traction motor is the main component of an electric vehicle. The motor converts the electrical energy into kinetic energy. This energy rotates the wheels. Electric motor is the main component that differentiates an electric car from conventional cars. An important feature of an electric motor is the regenerative braking mechanism. This mechanism slows down the vehicle by converting its kinetic energy into another form, and storing it for future use. There are basically two types of motors: DC and AC motors.

Power Inverter: It converts DC power from the batteries to AC power. Power inverter also converts the AC current generated during regenerative braking into DC current. This is further used to recharge the batteries.

Charging Port: The charge port connects the electric vehicle to an external supply. It charges the battery pack. The charge port is sometimes located in the front or rear part of the vehicle.

On-Board Charger: Onboard charger is used to convert the AC supply received from the charge port to DC supply. The on-board charger is located and installed inside the car. It monitors various battery characteristics and controls the current flowing inside the battery pack.

Controller: Power electronics controller determines the working of an electric car. It performs the regulation of electrical energy from the batteries to the electric motors.

Primary Battery: A lithium-ion battery is a type of rechargeable battery that has a higher energy density, high power-to-weight ratio, a long life, and is environmentally friendly which makes it better suited to consumer electronics than other commonly used rechargeable batteries like Ni-Cd, Ni-MH, and lead acid batteries. Batteries must be arranged in parallel and serial to form a battery pack for use in high-power applications such as electric vehicles and energy storage systems. Lithium-ion batteries perform safely and reliably when they are charged at the right rate, at the right temperature, or at the right voltage range. In excess of these limits, the battery's performance will quickly degrade, and there could even be safety issues.

Auxiliary Batteries: Auxiliary batteries are the source of electrical energy for the accessories in electric vehicles. In the absence of the main battery, the auxiliary batteries will continue to charge the car. It prevents the voltage drop, produced during engine start from affecting the electrical system.

Thermal Cooling System: The thermal management system is responsible for maintaining an operating temperature for the main components of an electric vehicle such as, electric motor, controller etc. It functions during charging as well to obtain maximum performance. It uses a combination of thermoelectric cooling, forced air cooling, and liquid cooling.

Transmission: It is used to transfer the mechanical power from the electric motor to the wheels, through a gearbox. The advantage of electric cars is that they do not require multi-speed transmissions. The transmission efficiency should be high to avoid power loss.

4.4 Location Selection and Data Analysis

In this Plug-in Hybrid solar and wind energy vehicle design the solar pane and the wind turbine are installed on the roof-top and the front of the vehicle respectively. For hybrid vehicle design, solar panels are typically placed on the car's roof because it receives direct sunlight. The car's roof has traditionally been the most suitable location for

installing solar panels. These solar roofs generate electricity that is used to run the car or some significant auxiliary equipment. Additionally, the batteries in the cars may be used to store energy so that it can be used to power some devices when there is no direct sunlight available, such as at night or on cloudy days.

The small horizontal axis wind turbine installs front of the car. The analysis shows that at a given speed, the front aerodynamic pressure of the vehicle is, its maximum value. The pressure drops on both sides of the wind turbine blade is greater when aerodynamic pressure is higher, this more pressure drop increasing the lift force. By accelerating the wind turbine's angular rotation with the help of this increased lift force, the generator can produce more electricity.

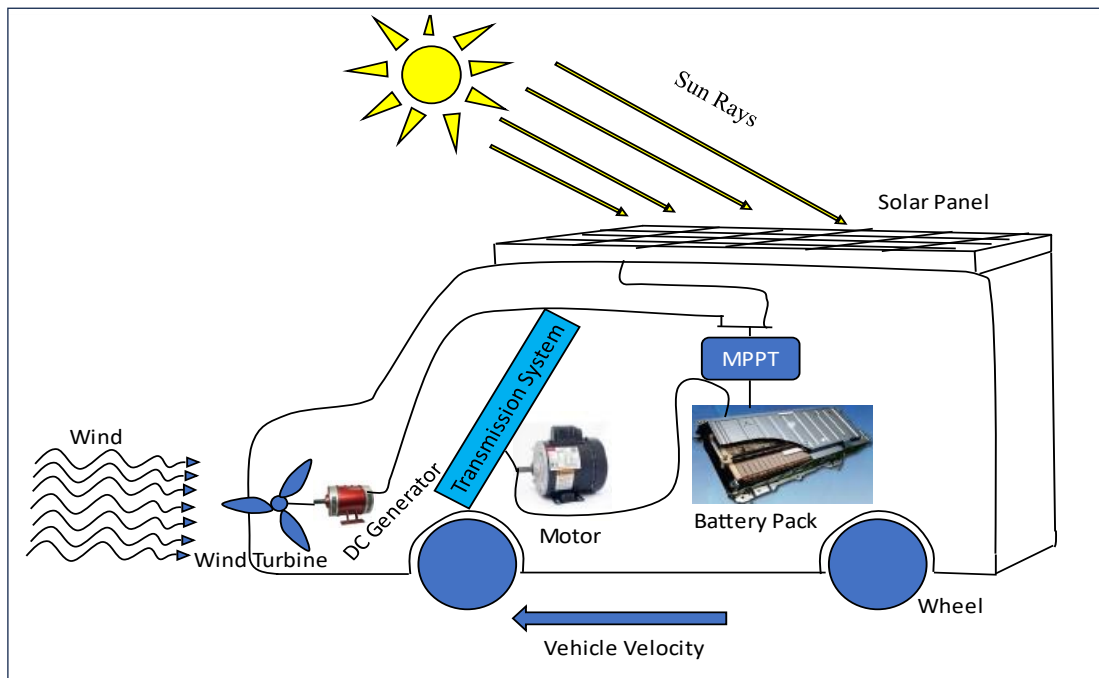


Fig. 8: Solar Panel and Wind Turbine position

Chapter 5

Design and Integration of Solar and Wind Energy System

5.1 Solar Panel Design and Placement

Solar energy is radiant light and heat from the Sun that is harnessed using a range of technologies such as solar power to generate electricity. Solar energy is the most abundant energy source of renewable energy emits from the Sun. It is an essential source of renewable energy, and its technologies are broadly characterized as either passive solar or active solar depending on how they capture and distribute solar energy or convert it into solar power. Active solar techniques include the use of photovoltaic system, concentrated solar power and solar water heating to harness the energy. Passive solar techniques include orienting a building to the Sun, selecting materials with favorable thermal mass or light-dispersing properties, and designing spaces that naturally circulate air.

Solar cars need solar arrays equipped with photovoltaic cells (PV cells) to convert sunlight into electricity. Unlike solar thermal energy that generates heat, PV cells directly turn sunlight into electric power by exciting electrons when exposed to solar photons. The most widely used material for PV cells is crystalline silicon, which typically has an efficiency rate ranging from 15% to 25%.

5.1.1 Fundamentals of Photovoltaic Technology

A solar cell is a device with the primary function of transforming solar light energy directly into electric energy through photovoltaic effect. Monocrystalline silicon, polycrystalline silicon, microcrystalline silicon, copper indium di-selenide and cadmium telluride are commonly used as semiconductors in photovoltaic systems. Selection of these materials is influenced by number of factors. PV system consists of many components like cells, module and arrays for generating power. In addition, various means of regulating and controlling structures, electronic devices, electrical

connections and mechanical devices are used for better operational efficiency. PV systems are rated in peak Kilowatts (kWp) which is an amount of electrical power delivered by a PV system when the sun is directly overhead in a clear day.

Based on different technologies and materials, the solar cells can also be grouped into 4 different generations:

First generation photovoltaic cell: The cell consists of a large-area, single-crystal, single layer p-n junction diode, capable of generating usable electrical energy from light sources with the wavelengths of sunlight. The cells are typically made using a diffusion process with silicon wafers. These silicon wafer-based solar cells are the dominant technology in the commercial production of solar cells, accounting for more than 86% of the terrestrial solar cell market.

Second generation photovoltaic cell: These cells are based on the use of thin epitaxial deposits of semiconductors on lattice-matched wafers. There are two classes of epitaxial photovoltaics – space and terrestrial. Space cells typically have higher AM0 efficiencies (28-30%) in production, but have a higher cost per watt. Their thin-film cousins have been developed using lower-cost processes, but have lower AM0 efficiencies (7-9%) in production. There are currently a number of technologies, semiconductor materials under investigation or in mass production. Examples include amorphous silicon, polycrystalline silicon, micro-crystalline silicon, cadmium telluride, copper indium selenide or sulfide. An advantage of thin-film technology theoretically results in reduced mass so it allows fitting panels on light or flexible materials, even textiles. Second generation solar cells now comprise a small segment of the terrestrial photovoltaic market, and approximately 90% of the space market.

Third-generation photovoltaics cell: They are proposed to be very different from the previous semiconductor devices as they do not rely on a traditional p-n junction to separate photogenerated charge carriers. For space applications quantum well devices (quantum dots, quantum ropes, etc.) and devices incorporating carbon nanotubes are being studied – with a potential for up to 45% AM0 production efficiency. For terrestrial applications, these new devices include photoelectrochemical cells, polymer solar cells, nanocrystal solar cells, Dye-sensitized solar cells and are still in the research phase.

Fourth Generation Photovoltaic cell: This hypothetical generation of solar cells may consist of composite photovoltaic technology, in which polymers with nano particles can be mixed together to make a single multispectrum layer. Then the thin multispectrum layers can be stacked to make multispectrum solar cells more efficient and cheaper based on polymer solar cell and multijunction technology used by NASA on Mars missions. The layer that converts different types of light is first, then another layer for the light that passes and last is an infra-red spectrum layer for the cell—thus converting some of the heat for an overall solar cell composite.

5.1.2 Working Principle of Solar Panel (PV Cell) System

The pure silicon with four valency crystals to uses in a solar panel to produce electricity form solar cells. The pure silicon ingots are reshaped and converted into very thin silicates called “silicon wafers”. The silicon wafer is the heart of PV cell. After the phosphorus atoms with five valency electrons are injected into silicon wafer. Here one electron if free to move. In this structure when the electron gets sufficient energy they will move freely, when sun light strikes them, the electrons will gain photon energy and will be free to move. However, this movement of the free electron is random. It does not result in any current through the load circuit. To make the electron flow unidirectional a driving force is needed. As easy and practical way to produces the driving force is a P-N junction. If P-type and N-type doping in pure silicon and then join together some electron from the N-region will migrate to the P-region and fill the holes available there. This way a depletion region is formed where there are no free electrons and holes. Due to electron migration the N-region boundary become slightly positive charged and P-region become negative charged. An electric field will definitely be formed between these charges. This Electric field produces the necessary driving forces. When light strikes the n-region of the PV cell and it penetrates and reaches up to the depletion region. This photon energy is sufficient to generated electron hole pairs in the deflection region. The electric field in the depletion region drives the electron and holes out of the depletion region. Here we observe that the concentration of electron in N-region and holes in P-region become so high that a potential difference will develop between them. As soon as we connect any load between these regions, electron will recombine with the holes in the P-region after completing their path. In a practical solar cell, you can see that the top N-layer is very thin and heavily doped, where the P-

layer is thick and lightly doped. In this design depletion area are much more, so that due to the light-striking the electron hole pairs are generated in a wider area compared to the previous case. This results in more current generation by the PV cell. The other advantage is that due to the thin top layer, more light energy can reach the depletion region.

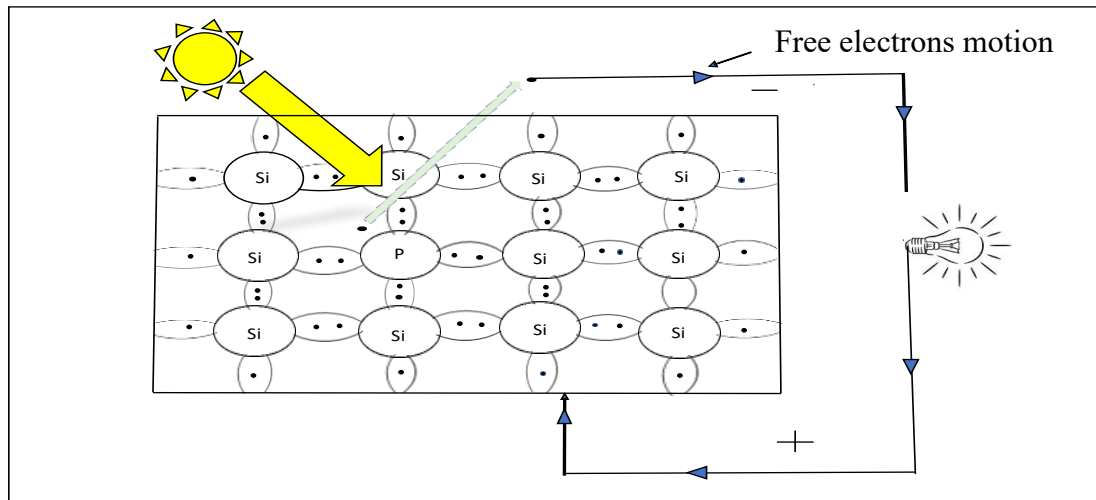


Fig. 9: Working Process of Solar Panel

5.1.3 Monocrystalline PV Solar Cell

Monocrystalline solar panels, also known as single-crystalline silicon panels, are made from a single silicon crystal, typically cylindrical in shape. These panels connect individual silicon cells in series, ensuring high purity for increased efficiency while managing costs. Unlike polycrystalline panels, monocrystalline panels are cut from a single silicon piece, making them more efficient. Monocrystalline solar cells are cut from a single piece of silicon, making them more efficient than polycrystalline panels. Monocrystalline solar panels are also known for their dark black hue on their surface.

Type of monocrystalline Solar panel:

There are various types and capacities in monocrystalline solar panel, mainly there are two type of monocrystalline solar panel that are Mono PERC solar panel and Bifacial solar panel.

Mono PERC Solar Panel: PERC monocrystalline solar panel is the latest technology and powerful solar panel. Mono PERC solar panel are usually expensive than other type

of solar panel but they have a longer lifetime and the better performance in low-light condition. It uses PERC cells which are considered to be the latest invention in the solar field. PERC stands for Passivated Emitter and Rear Contact. This technology is invented to achieve higher power conversion efficiency by adding a dielectric passivation layer on the rear of the cell. Besides, the PERC technology saves your cells' performance by preventing longer wavelengths from becoming heat and justifying the rear combination.

First introduced in 1989, PERC panels are modified silicon cells that have an additional layer on the back. Because this extra layer is reflective, it is able to send unused light back across the N-type and P-type junctions to generate more energy. Better still, this reflective surface also helps to reduce rear recombination and prevent longer wavelengths from becoming heat that would otherwise impair the cell's performance. With steady improvements over the years, PERC modules have since achieved solar generation efficiencies up to 12% higher than their traditional silicon counterparts. We can install a PERC module even on a small roof. A high-efficiency PERC solar module can reduce installation time and costs while increasing power production significantly.

Working Function of Mono PERC solar panel:

The sunray enters the solar panel and passes through the protective glass and encapsulant then the sunlight encounters a level of anti-reflecting coating that increase the amount of sunlight absorbed by monocrystalline solar panel. The photons of sunlight are absorbed by the single silicon atoms in the p-n junction create an electric field. The electric create the free electrons in the n-type silicon to move towards the P-N junction and the holes in the p-type silicon to move away from the P-N junction. Then the movement of the electrons and the holes creates a flow of electrical current. The produce electricity is collected by a conductive metal wires on the surface of the solar panel and stored into the battery pack.

Details of Mono PERC solar Panel cell:

Protective Glass: When choosing a solar panel, people often consider elements such as the solar PV panel's power and overall efficiency. However, they may not consider how

the type of solar panel glass influences performance. The glass also plays a key role in protecting the panel's photovoltaic cells against environmental factors.

It's important not to overlook solar panel glass when looking for the ideal solar panel model. Here we'll go over what options to look for and what they can do for your solar panels.

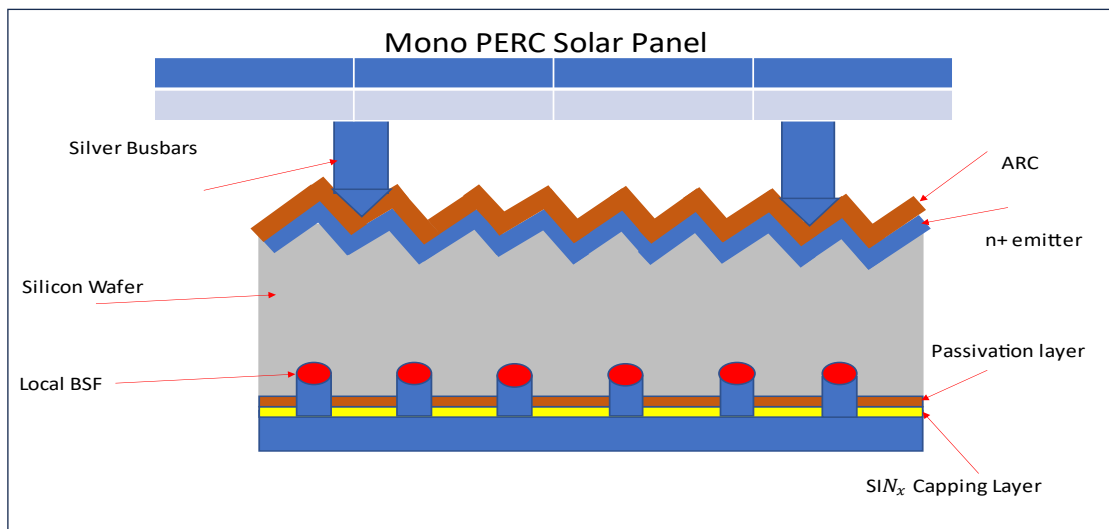


Fig. 10: Schematic diagram of Mono PERC Solar Panel

Types of Solar Panel Glass:

Solar panel glass may consist of two main types: thin-film or crystalline. Both have distinct features to keep in mind.

Thin-Film — Thin-film glass is lightweight, cost-effective, and easy to install. They are made of standard, non-tempered glass and can be as thin as 2.5 mm. Thin-film solar panels are lightweight because the glass encloses the panel without a frame. They require the most space and have the lowest efficiency out of all the solar panel glass options.

Crystalline — Solar panels made with crystalline glass tend to have a thickness of 3 to 4 mm, which adds more stability. This glass has a unique rough surface, which enables the glass to bond well with the panel's EVA film for lamination purposes. Smooth glass can lead to gradual delamination. There are two subtypes of crystalline glass: monocrystalline and polycrystalline. Both of these crystalline panels require a

fabrication method that involves producing silicon crystals that are cut into thinner wafers for use in solar panel glass.

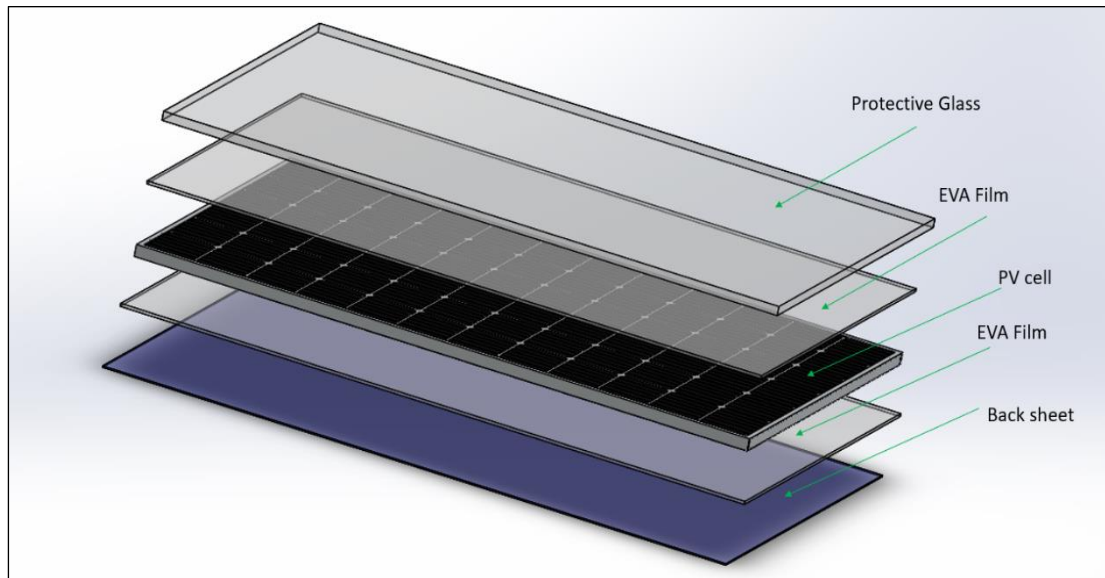


Fig. 11: Different layers of a Solar Panel

Monocrystalline — These panels feature a sleek look and optimal efficiency, but they're slightly more expensive than polycrystalline glass.

Polycrystalline — These are less expensive than their monocrystalline counterparts, at the cost of reduced visual appeal and efficiency.

Function of Solar Panel Glass:

Solar panel glass performs a few main functions for solar panels, including:

Protection from damage — Tempered solar panel glass serves as a protective layer for solar panels, preventing environmental factors like vapours, water, and dirt from damaging the photovoltaic cells. Tempered solar panel glass also provides high strength, excellent transmissivity, and low reflection.

Durability and safety — Tempered glass offers up to four times more strength than standard glass. This strength is critical as the solar panel's front sheet requires lasting protection against the elements. Thanks to the thermal and chemical processes that produce tempered glass, it is also known as toughened or safety glass. Tempered glass is safer to use because it shatters into many smaller pieces when broken, reducing the probability of accidental injury.

Weight — Glass must be of a certain weight for solar panels. The industry standard weight for a 3.2 mm thick solar panel glass is around 20 kg. Tempered glass can provide this minimum weight, avoiding the dangers of cheap, lightweight solar panel glass.

EVA Film – Ethylene-vinyl acetate (EVA), a copolymer of ethylene and vinyl acetate, is widely used as an encapsulant in the silicon solar module to bind the different layers together and protecting the solar cells from over stressing, cracking, and environmental effects. In this work, EVA has been recovered successfully from the used silicon solar module by thermal treatment at 170°C temperature and the application of mechanical force. The established process is completely environment-friendly, as the EVA layer was recovered without any degradation and emission of any gas. the material widely used for the encapsulation of solar cells is EVA (ethylene–vinyl acetate), which is a copolymer of ethylene and vinyl acetate, having a 10–40% weight percentage of the vinyl acetate with remaining ethylene material. EVA is a low-cost material having good adhesion, good chemical, and physical characteristic for silicon solar module encapsulation. Usually, a thin (0.5 mm) transparent film of polymer is used for encapsulation so that they can maintain better optical transmission (90%) in a prescribed spectral region.

Backsheet – The PV Backsheet material chosen for solar panel will have a considerable impact on how it withstands the elements and performs over the course of its lifetime. A reliable backsheet should be able to provide protection from moisture, physical damage and UV rays, while also minimizing electrical discharge and thermal degradation. The active electrical elements found within the modules must also be insulated to ensure the safety of surroundings. The PV backsheet material is layered atop an encapsulant on the solar cell. Backsheet is a film that protects the solar cell from severe environmental conditions. A solar backsheet is the last layer at the bottom of the solar PV panel and is typically made of a polymer or a combination of polymers. One of the less visible but essential components of a solar panel to their long-term performance in backsheets.

Bifacial Mono Crystalline Solar Panel: Bifacial modules produce solar power from both sides of the panel. Whereas traditional opaque-backsheeted panels are mono-facial. Bifacial modules expose both the front and backside of the solar cells. The

average efficiency of a bifacial panel is 11 to 12% more than a traditional panel.

Working Principle of Bifacial Mono Crystalline Solar Panel:

As already mentioned, Bifacial modules have two faces to gather sunlight. They work as follows.

The Front Face: In a bifacial solar panel system, the panel top is equipped with solar cells facing the sun. This side of the panel works similar to a common solar panel capturing the Sun rays directly coming from the sun. The incident rays are collected here consuming only certain wavelengths.

The Rear Face: The solar cells present on the other face, the bottom face, absorb the reflected light off the ground. With proper instalment comes a great amount of reflection which in turn increases the bifacial solar panel efficiency manifold.

In solar panel design bifocal mono-crystalline solar panel is not suitable because the rear part of solar panel doesn't generate any energy due to covered. So, in this solar design used PERC mono-crystalline solar panel in this vehicle design.

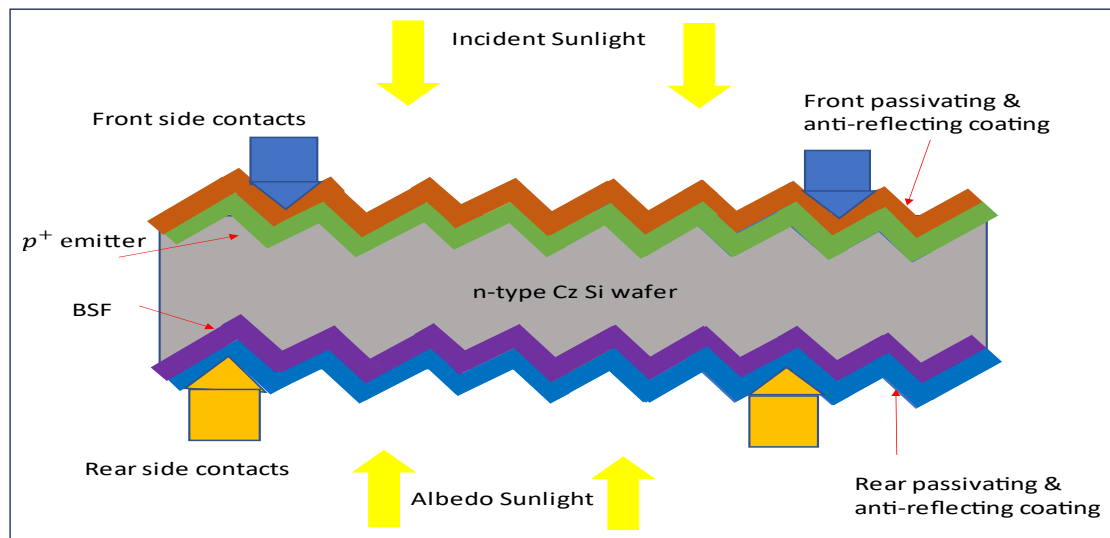


Fig. 12: Schematic diagram of Bifacial Mono PERC Solar Panel

5.2 Wind Turbine Design and Placement

The main components in the wind turbine are rotor blades (in our design 3 blades), electromagnetic brakes, mechanical brakes, gearbox, shaft, generator, different

controller system likes yaw drive, pitch angle controller, rotation speed, wind direction etc.

Rotor Blades: Lifts and rotates when wind is blow over the blades, causing the rotor to spin. Most of the wind turbine have either two or three blades.

Controller: Starts up the machine at wind speeds of about 8 to 16 miles per hour (mph) and shuts off the machine at about 55 mph. Turbines do not operate at wind speeds above about 55 mph because they may be damaged by the high winds.

Gear Box: Connects the low-speed shaft to the high-speed shaft and increases the rotational speeds from about 30-60 rotations per minute (rpm), to about 1,000-1,800 rpm; this is the rotational speed required by most generators to produce electricity.

Wind vane: Measures wind direction and communicates with the yaw drive to orient the turbine properly with respect to the wind.

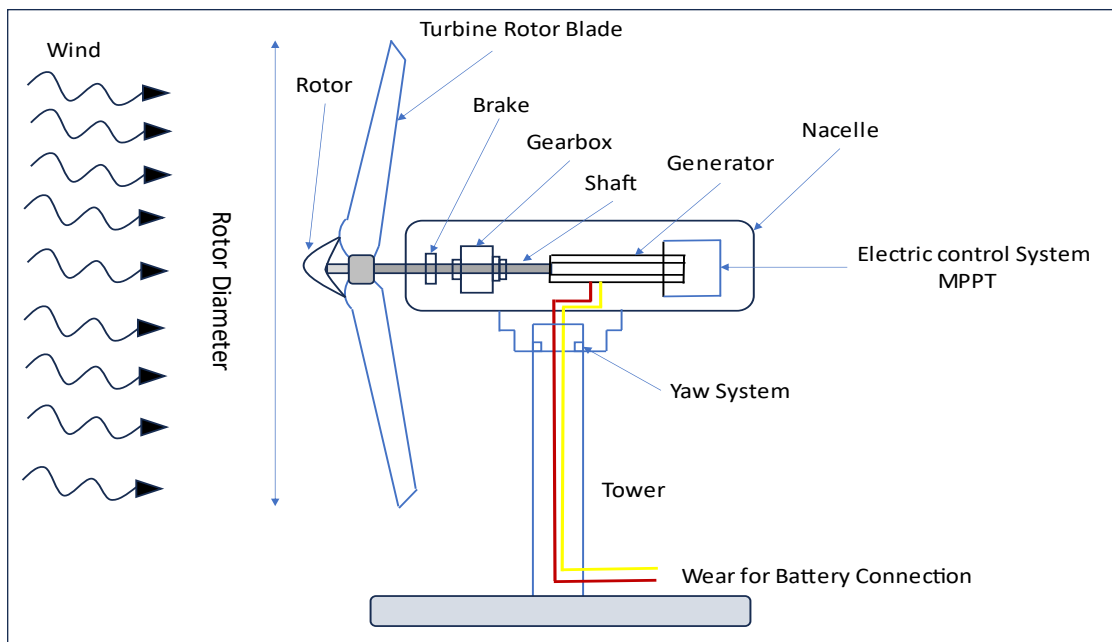


Fig. 13: Schematic diagram of different parts of Wind Turbine

Generator: Produces 50-cycle AC electricity using the rotor rotation. Usually, the small wind turbines tend to use a low-speed permanent magnet DC generator or Dynamo as they are small, cheap and a lot easier to connect up.

Mechanical System of Wind Turbine:

Rotor Blade Design: The rotor blades have two basic functions; one is they have to generate optimal aerodynamic forces that make the wind turbine blade turn, another is the rotor blade have to convert the kinetic energy of the wind in rotational mechanical energy. The rotor blade thus has to deliver light weight and high aerodynamical performance and also to provide enough strength and stiffness in order to meet maximum efficiency.

Blade Twist: The advantages of a curve rotor blade compare to the flat blade is that lift forces allow the blade tips of the wind turbine to move faster than the wind is moving generating more power and increasing the overall efficiency.

Effect of the number of blades: Increasing the number of blades results in increasing the aerodynamics efficiency of turbine. Increasing the number of blades from one to two results in a six-percent increasing aerodynamic efficiency, whereas increasing the number from two to three yields only an additional three-percent. Further increasing number of blades results very small percentage increasing the efficiency. So, for optimal efficiency we used three blades.

Blade length: Power proportionally related to the square of the blade length. A longer blade will favour the power extraction.

Working Principle of Wind Turbine:

Turbines use blade designs similar to airplane wings to capture the kinetic energy of the wind. When the wind blows, it creates a low-pressure area on one side of the blade, pulling it in that direction and causing the rotor to turn due to lift force. Lift force is stronger than the wind's force on the front side of the blade, known as drag force. These forces together make the rotor spin, much like a propeller. The wind turbine blade connects to a gearbox through a rotor shaft, which, in turn, is connected to a generator via a high-speed gearbox. A series of gears increase the rotation of the rotor in a certain speed that allow the turbine generator to produces AC electricity. This produced AC current converted DC by a converter then store battery through a MPPT system. A streamlined enclosure called a nacelle houses key turbine components, usually including the gears, rotor and generator, low- and high-speed shafts and controller

system are found within a housing called the nacelle. Orients upwind turbines to keep them facing the wind when the direction changes. The main purpose of the yaw drive mechanism arrangement is to move the nacelle and blades according to the wind direction. It enables the wind turbine to capture the maximum available wind. During the nacelle movement, a fair chance of cable twisting occurs inside the tower. A brake, also housed in the nacelle, stops the rotor mechanically, electrically or hydraulically in emergencies.

Wind Turbine Design: In wind turbine blade design using a very popular air foil is NACA 2414. In this wind turbine design uses three blades to get the maximum power output. The rotor diameter of the blade is 255 mm and the swept area of the wind turbine is 0.2042 m^2 . Using material of wind turbine blades design is carbon fiber. Wind turbine containing carbon fiber weight 25% less than ones made from traditional fiberglass materials. And also, carbon fiber can capture more energy in location with low wind speed and this blade lifetime could be longer than fiberglass ones because this material have a high fatigue resistance.

Table 2: Horizontal Axis Wind Turbine Blade Design Parameter

Rotor Radius(mm)	Chord Length (mm)	Twist Angle (°)
60	137.94	-25
120	110.23	-25
180	77.25	-20
255	59.63	-20

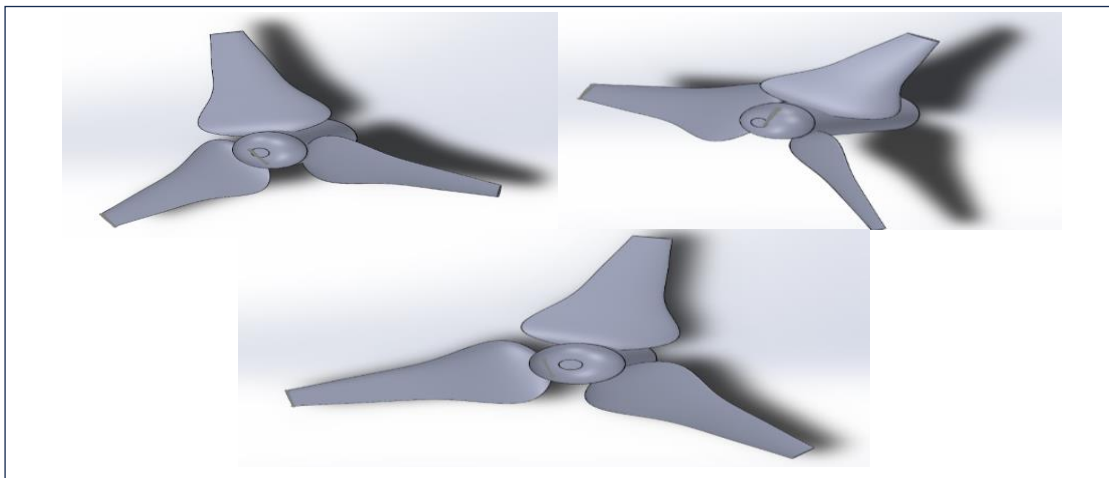


Fig. 14: Small Horizontal Axis Wind Turbine

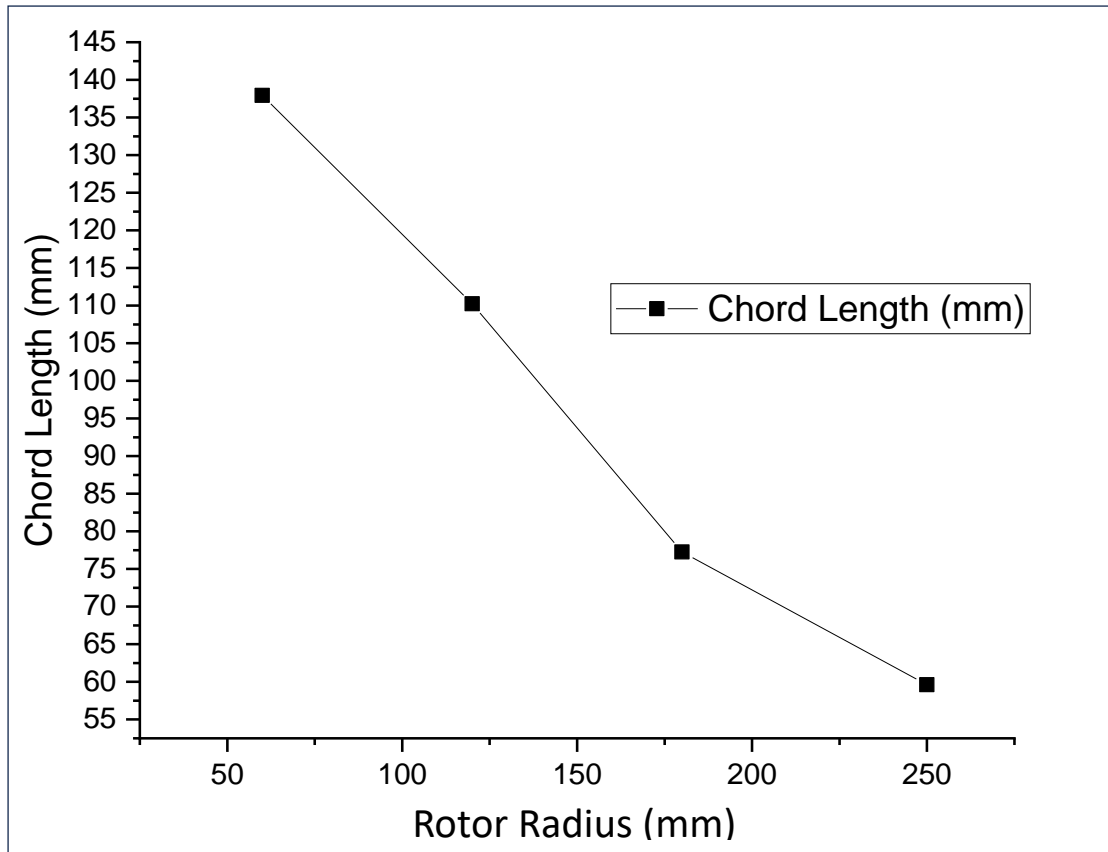


Fig. 15: Wind Turbine Blade Chord Length Vs. Rotor Radius

5.3 Integration of Solar and Wind Systems

With the aim of building an energy-efficient, financially stable, and generally sustainable society, plug-in hybrid electric vehicles (PHEVs) with solar and wind power system are currently being heavily promoted as a competitive alternative to both conventional and regular hybrid electric vehicles. In this analysis designed a solar and wind power mounted plug-in hybrid electric vehicle. A monocrystalline PERC silicon solar cell used for the producing electric energy directly from the sunlight. A small horizontal axis wind turbine used for the producing electric energy by using generator when the vehicle on a motion with a certain speed. The solar and wind power system series connected with battery pack by through MPPT charge controller system.

5.4 Energy Conversion and Storage Systems

After producing electric energy from the solar and wind energy system this energy stored a lithium-ion battery. A lithium-ion battery is a type of rechargeable battery that

has a higher energy density, high power-to-weight ratio, a long life, and is environmentally friendly which makes it better suited to consumer electronics than other commonly used rechargeable batteries like Ni-Cd, Ni-MH, and lead acid batteries. Lithium-ion batteries perform safely and reliably when they are charged at the right rate, at the right temperature, or at the right voltage range. In excess of these limits, the battery's performance will quickly degrade, and there could even be safety issues.

Auxiliary batteries are the source of electrical energy for the accessories in electric vehicles. In the absence of the main battery, the auxiliary batteries will continue to charge the car. It prevents the voltage drop, produced during engine start from affecting the electrical system.

Chapter 6

Performance Analysis

6.1 Efficiency Analysis

The efficiency of plug-in hybrid electrical solar and wind power systems is affected by the performance of the solar panels and wind turbines, as well as the battery capacity, battery efficiency, solar and wind turbine charging controller MPPT system, motor controller, and other factors. The efficiency of the hybrid vehicle depends on the series and parallel connection of the solar panel output energy and wind turbine power output energy. The battery, a crucial element of the design, plays the most significant role in an electric vehicle's efficiency performance analysis. For electric cars right now, lithium-ion batteries are the best choice. The analysis of a vehicle's battery efficiency also considers the range of the vehicle.

6.2 Vehicle Performance Evaluation

Solar and wind power with plug-in hybrid vehicle performance depend on several things. At the day time the solar power system can properly work but at night they cannot produced any electricity. The energy conversion of solar panel is depended on the weather condition, inside interior temperature of the vehicle, atmospheric temperature, inclination angle and hour angle etc. The power output from the wind turbine is affected by the wind velocity, wind velocity direction, vehicle speed and also the relative velocity of the wind and vehicle. Also, wind turbine power output is directly proportion to how much times a vehicle moved per day. The hybrid electric vehicle power consumption is depended on the shape of the vehicle. The power consumption is less when the drag coefficient of the vehicle is minimum. So, in this chapter analysis several factor that can make some effect on vehicle performance.

6.2.1 Weather Condition on the Solar Panel System

Outside atmosphere condition make maximum effect on the solar power system. At the day time only, the solar panel system can produce useful electricity. Photovoltaic (PV) solar panels can generate electricity from both direct and indirect sunlight. This suggests that they are still capable of working while the cloud is active. However, on sunny days, when they are exposed to direct sunlight, solar panels perform at their peak efficiency. Solar panels continue to work even when the sun's rays are partially or completely blocked by clouds, but their capacity to generate energy is diminished. Solar panels typically generate 10 to 25% less power than usual on days with a lot of cloud cover. Rain is typically a byproduct of clouds, and here's something you might not be expecting, rain makes solar panels more efficient. This is due to the fact that rain removes any dirt or dust buildup from your panels, allowing them to absorb sunlight more efficiently.

Extreme Summer Day

Solar panels work well in a wide range of weather conditions. However, it's a common misconception that hot climates are best for solar panel performance. Solar panels operate more effectively in colder climates, producing more voltage and, consequently, more electricity, similar to other electronics. As the temperature rises, the panel produces less voltage and works less effectively, producing less electricity. Even though the amount of power a solar panel produces is directly related to the amount of sunlight it receives. This loss is displayed as a temperature coefficient versus power on the datasheet provided by the manufacturer.

Cold Winter Day

The photovoltaic panels generate electricity from sunlight, not from outside air temperature. As a result, the panels will work even in extremely cold weather. The fact that the sun rises every day in cold climates means that solar power can be used even when the temperature is extremely low.

6.2.2 Vehicle Speed effect on the Wind Turbine System

Aerodynamics of Wind Turbine Blade: A wind turbine turns wind energy into electricity using the aerodynamic force from the rotor blades. When wind flows across the blade, the air pressure on one side of the blade decreases. The difference in air pressure across the two sides of the blade creates both lift and drag force. The lift force is stronger than the drag force and this causes the rotor to spin.

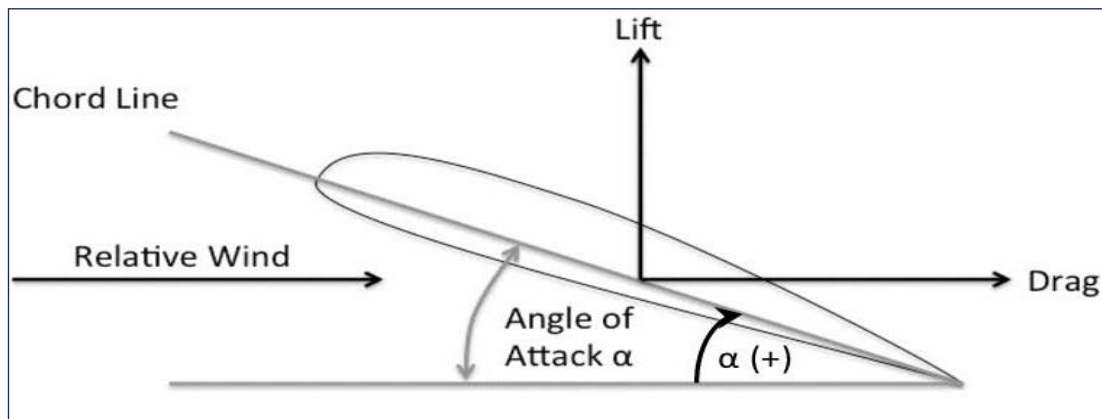


Fig. 16: Drag and Lift Force at an Alpha Angle of Attack

$$Pressure + \frac{Kinetic\ Energy}{Volume} = Constant$$

$$P + \rho gh + \frac{1}{2}\rho v^2 = Constant$$

Where, P is the static pressure (in N/m²), h is the elevation and g is the gravitation acceleration.

Drag Force and Lift Force:

The force parallel to the direction of motion is called drag force. Drag is a loss that must be overcome with another force, if an object is to move against a stream. The moment around this axis is called a rolling moment.

$$D_d = \frac{1}{2} \times C_d \times \rho \times w^2 \times c \times dr$$

Where,

D_d = Drag force

C_d = Drag coefficient

W = Relative air speed

C = Blade cord length

r = Blade radius

The force perpendicular to the direction of motion is called lift force. This force very essential for wind turbine. The lift force can be determined as,

$$D_L = \frac{1}{2} \times C_L \times \rho \times w^2 \times c \times dr$$

Where,

D_L is the Lift force

C_L is the Lift coefficient

Tip Speed Ratio and Solidity:

Tip speed ratio is one of the most important factors to design the wind turbine blade. TSR refers to the ratio between the speed of the tips of the wind turbine blades and the wind speed.

$$\text{TSR, } \lambda = \frac{\text{Tip speed of blades}}{\text{Wind speed}} = \frac{\pi D n}{60 v}$$

Where,

λ = Tip speed ratio

D = Rotor diameter (m)

n = Rotor rotational speed (rpm)

v = Wind velocity (m/s)

Solidity is the ratio of total rotor platform area to the total swept area.

$$\text{Solidity} = \frac{3a}{A}$$

Where, a is the total rotor platform area and A is the total swept area.

Betz Limit: The Betz limit is the theoretical maximum efficiency for a wind turbine, conjectured by German physicist Albert Betz in 1919. Betz concluded that this value is 59.3%, meaning that at most only 59.3% of the kinetic energy from wind can be used to spin the turbine and generate electricity. In reality, turbine cannot reach the Betz limit, and common efficiencies are in the 35-45% range.

6.3 Energy Generation and Consumption Analysis

6.3.1 Solar Energy Generation

The total amount of radiation calculated for a particular location or area is given as global radiation. The calculation of direct, diffuse, and global insolation is repeated for each feature location or every location on the topographic surface, producing insolation maps for an entire geographic area. Solar insolation units are normally kWh/m²/day, which represents the daily amount of solar energy in kilowatt hour striking a square meter area on the earth's surface.

Hour Angle (ω): Hour angle is calculated using this formula -

$$\omega = \frac{360(T - 12)}{24}$$

Where, T is any time of a day.

Time equals hour of day from midnight Zenith angle (Z) is calculated using formula:

$$Z = \cos^{-1}(\sin\phi\sin\theta + \cos\phi\cos\theta\cos\omega)$$

Zenith Angle: The angle from the point directly overhead to the point of the sun's position in the sky. Where ϕ is latitude, θ is solar declination angle and ω is the hour angle. Solar declination angle is the angle between the perpendicular plane to incoming solar radiation and the earth's rotational axis. The solar declination angle varies from +23.5° (degree) on summer solstice to -23.5° (degree) on winter solstice, and 0° (degree) on the vernal equinox and autumnal equinox.

Declination Angle (δ): The declination angle, denoted by δ , varies seasonally due to the tilt of the Earth on its axis of rotation and the rotation of the Earth around the Sun. If the Earth were not tilted on its axis of rotation, the declination would always be 0° . However, the Earth is tilted by 23.45° and the declination angle varies plus or minus this amount. Only at the spring and fall equinoxes is the declination angle equal to 0° . The rotation of the Earth around the sun and the change in the declination angle is shown:

The declination angle can be calculated by the equation:

$$\delta = 23.45^\circ \times \sin\left(\frac{360(d + 284)}{365}\right)$$

Where, d is the day of the year with Jan 1 as $d=1$, Jan 2 as $d=2$,, Dec 31 as $d=365$.

Table 3: Number of days variation with date

Month Name	'd' for the Day of month
January	i
February	31+i
March	59+i
April	90+i
May	120+i
June	151+i
July	181+i
August	212+i
September	243+i
October	273+i
November	304+i
December	334+i

Where, 'i' is the number of the day 1 to 31 of the particular month.

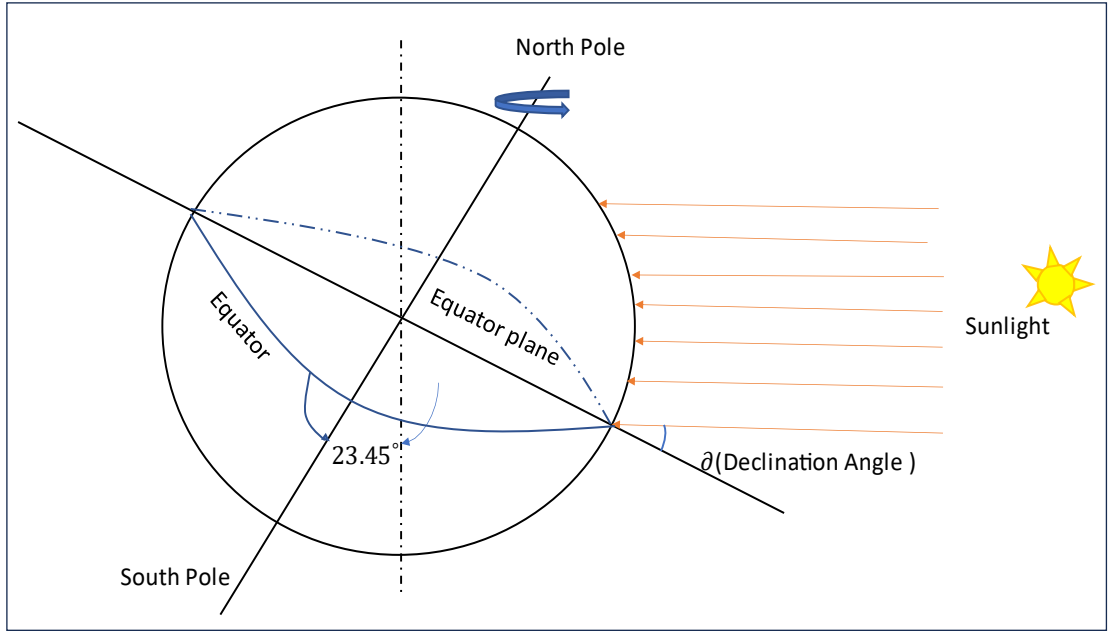


Fig. 17: Solar Ray inclination Angle (θ°) on Earth Surface

Tilt Angle (β): Tilt Angle is the angle between the horizontal plane and the solar panel at which can be set or adjusted to maximize seasonal or annual energy collection.

PV modules should ideally be tilted at an angle that's equal to the site's latitude. However, the panels will often be attached to a roof and will follow that angle instead. This may not always be ideal, but it will be the most practical and affordable and, in most cases, will still produce good results. If a roof is flat, a tilt frame might also be used to get the angle closer to the latitude. Having some tilt to the panels also means that they'll be cleaned when it rains.

In this analysis value of tilt angle is zero ($\beta = 0$).

Incidence Angle (θ): The solar incidence angle(θ), is the angle between the sun's rays and the normal on a surface. For a horizontal plane, the incidence angle, θ , and the zenith angle (Z) are the same. The Equation of Incidence angle is:

$$\cos \theta = \sin \delta \sin \phi \cos \beta - \sin \delta \cos \phi \sin \beta \cos Z + \cos \delta \cos \phi \cos \beta \cos \omega + \cos \delta \sin \phi \sin \beta \cos Z \cos \omega + \cos \delta \sin \beta \sin Z \sin \omega$$

Where,

δ is the declination angle of solar ray

ϕ is the latitude angle of the analysis area

Z is the sun zenith angle in the analysis area

ω is hour angle

β is the solar panel surface tilt angle from the horizontal

In this analysis the value of sun zenith angle (Z) is zero (0°) and for the horizontal surface the value of the solar panel surface tilt angle (β) also zero (0°), so the value of incidence angle:

$$\cos \theta = (\sin \delta \sin \phi \cos 0 - \sin \delta \cos \phi \sin 0 \cos 0 + \cos \delta \cos \phi \cos 0 \cos \omega + \cos \delta \sin \phi \sin 0 \cos 0 \cos \omega + \cos \delta \sin 0 \sin 0 \sin \omega)$$

$$\cos \theta = \sin \delta \sin \phi + \cos \delta \cos \phi \cos \omega$$

In our location on 15 May at 12 P.M., the value of hour angle (ω) is zero (0°), the value of the declination angle of sun ray is $\delta = -18.79^\circ$ and the latitude angle is $\phi = 22.61^\circ$.

$$\cos \theta = \sin(-18.79) \sin(22.61) + \cos(22.61) \cos(-18.79) \cos 0$$

$$\cos \theta = -0.1238 + 0.8682$$

$$\cos \theta = 0.744$$

$$\theta = \cos^{-1} 0.744$$

$$\theta = 41.85^\circ$$

So, the Incidence angle of the month of June is at Kolkata is $\theta = 41.85^\circ$.

Now, the atmospheric transmittance for beam radiation equation,

$$\tau_b = a_0 + a_1 \exp\left(\frac{-k}{\cos \theta}\right)$$

The constant a_0 , a_1 and k for the standard atmosphere with 23 km visibility are found from a_0^* , a_1^* and k^* which are given for altitudes less than 2.5 km by

$$a_0^* = 0.4237 - 0.00821(6 - A)^2 = 0.331$$

$$a_1^* = 0.5055 + 0.00595(6.5 - A)^2 = 0.594$$

$$k^* = 0.2711 + 0.01858(2.5 - A)^2 = 0.271$$

Table 4: Climate correction factors at different season of Year

Climate Type	r_0	r_1	r_k
Tropical	0.95	0.98	1.02
Midlatitude Summer	0.97	0.99	1.02
Subarctic Summer	0.99	0.99	1.01
Midlatitude Winter	1.03	1.01	1.00

Now, correction factors are applied

$$a_0 = r_0 \times a_0^* = 0.97 \times 0.331 = 0.321$$

$$a_1 = r_1 \times a_1^* = 0.99 \times 0.594 = 0.588$$

$$k = r_k \times k^* = 0.271 \times 1.02 = 0.276$$

Now,

$$\tau_b = 0.321 + 0.594 \exp\left(\frac{-0.276}{\cos 41.85}\right) = 0.731$$

The value of the constant is approximately $I_{SC}=1.366$ kilowatts per square metre. Value of solar constant at a particular day is,

$$I_{SC}' = I_{SC} \left[1 + 0.033 \times \cos\left(\frac{360 \times d}{365}\right) \right] \times \tau_b$$

The value of solar constant at 15 May is:

Value of $d=135$

$$I_{SC}' = 1366 \left[1 + 0.033 \times \cos\left(\frac{360 \times 135}{365}\right) \right] \times 0.731 = 976.12 \text{ W/m}^2$$

The solar panel efficiency calculation formula is,

$$\eta = 0.28 - 0.001 (T_{cell})$$

From the analysis, the solar panel cells average temperature is found to be (T_{cell}) 64.85° . So,

$$\eta = 0.28 - 0.001(64.85) = 0.215$$

$$\eta = (0.215 \times 100) \% = 21.5 \%$$

Output Electric Energy Calculation of Solar Panel:

Area of the single solar panel is $A = 0.1 \times 0.2 = 0.02 \text{ m}^2$

Number of solar cells is 144.

So, the total area of solar panel is $A = 0.02 \times 144 = 2.9 \text{ m}^2$

Total amount of the solar radiation energy incident on the solar panel protective glass is 976.12 W/m^2 . The efficiency of the solar panel protective glass is approximately 90%. So, the solar energy pass through the protective glass:

$$976.12 \times 0.9 = 878.508 \text{ W/m}^2$$

This amount of solar energy incident on the EVA part of solar panel. The efficiency of EVA system is 78.5%. Solar radiation energy pass through the EVA:

$$878.508 \times 0.785 = 689.62 \text{ W/m}^2 \text{ and incident on the solar cell.}$$

From the analysis we find the efficiency of solar cell is 21.5%. The final amount solar radiation energy convert into electric energy by the solar panel is -

$$E' = 689.62 \times 0.215 = 148.27 \text{ W/m}^2$$

So, the overall efficiency of solar panel is $= \frac{148.27}{968.93} \times 100 = 15.18\%$

The amount of electric energy creates by the design solar panel per day,

$$E = E' \times \text{Sun hour} \times 0.75 \text{ W/m}^2 = 148.27 \times 10.5 \times 0.75$$

$$E = 1167.627 \text{ W/m}^2 = 1.1676 \text{ kW/m}^2 \text{ per day}$$

The amount of energy at per meter square area, $E = 1.1676 \text{ kW/m}^2$

Solar panel total area is 2.9 m^2

The value of total electric energy of the design solar panel is $1.1676 \times 2.9 = 3.38 \text{ kW}$ per day.

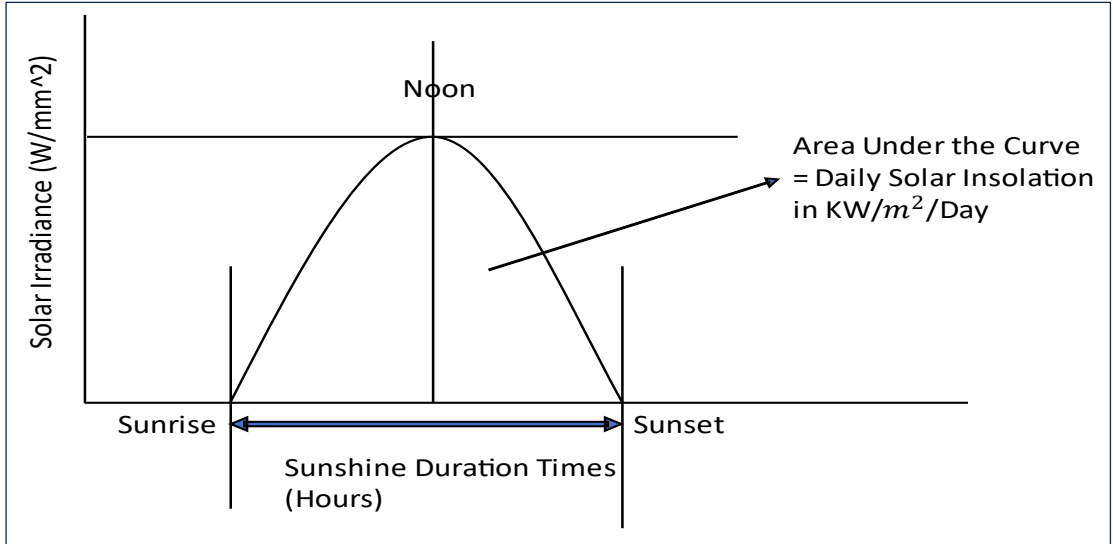


Fig. 18: Graph of Solar Irradiance Vs. Hour Angle

6.3.2 Solar Panel Voltage and Current Analysis

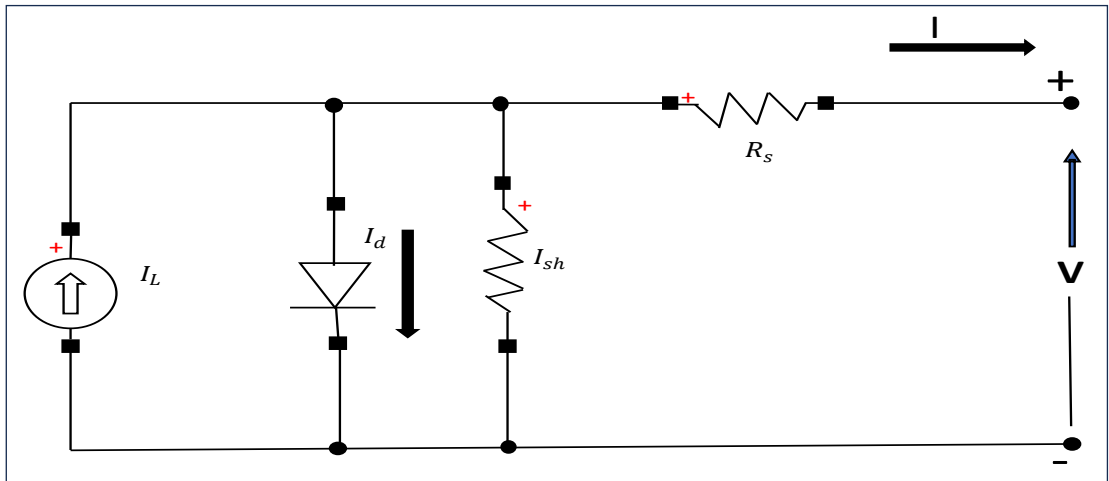


Fig. 19: Solar Cell Electric Circuit

The PV array block implements an array of photovoltaic (PV) modules. The array is build of strings of Modules connected in parallel, each sting consisting of modules connected in series. In every stings 24 solar cell connected in series and 6 string connected in parallel. Total number of small solar cell is 144. The PV array block is a five paramenter model using a current source I_L (light-generated current), diode (I_0 and nl parameter), series resistance R_s and shunt resistance R_{sh} to represent the irradiance and temperature- dependent I-V characteristics of the solar modules.

The diode I-V characteristics for a single module are repretens by the equations:

$$I_d = I_0 \left[\exp \left(\frac{V_d}{V_T} \right) - 1 \right]$$

$$V_T = \frac{kT}{q} \times nl \times N_{cell}$$

Where,

I_d = Diode current (A)

V_d = Diode voltage (V)

I_0 = Diode saturation current (A)

nl = Diode ideality factor, a number close to 1

k = Boltzman contant = $1.3806 \times 10^{-23} \text{ J.K}^{-1}$

q = Electron charge = $1.6022 \times 10^{-19} \text{ C}$

T = Cell temperature (K)

N_{cell} = Number of cell connected in series in a module

6.3.3 Wind Turbine Aerodynamic Analysis

Wind turbines are mainly utilized for the purpose of producing electricity from the wind. Aerodynamics plays a significant role in the operation of wind turbines. As with most other machines, wind turbines come in a wide variety of designs and are all built on different theories for obtaining energy. The aerodynamic movement of the rotor blades is responsible for harnessing wind power to generate electricity. One side of the blade experiences a decrease in air pressure when wind passes through it. The difference in atmospheric pressure between the two sides results in the creation of lift and drag forces. As the lift force exceeds the drag force, causing the rotor to rotate.

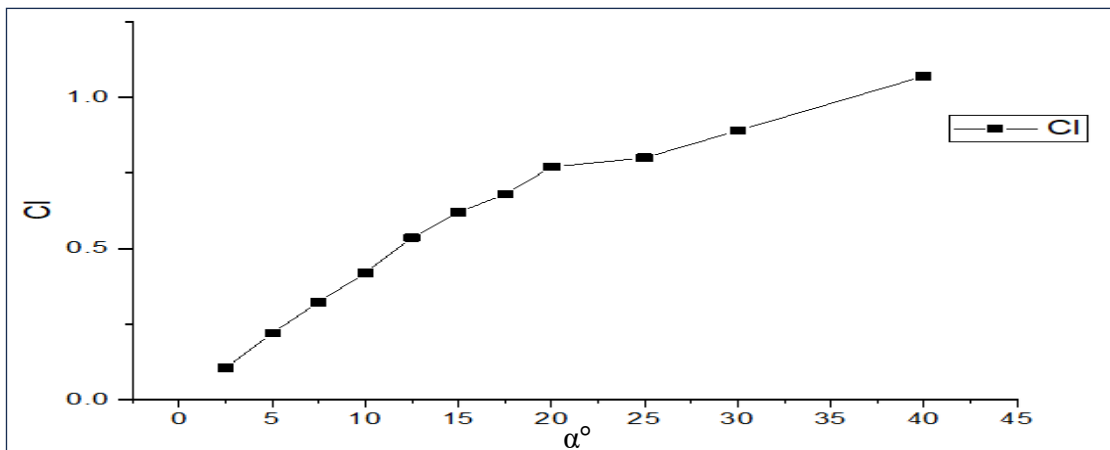


Fig. 20: Graph between Lift Coefficient and AOA (α°)

In a standard graph depicting the coefficient of lift versus the angle of attack (AOA) for an airfoil section analysis, we observe that the lift coefficient increases as the angle of attack rises. However, beyond a specific AOA angle, the lift coefficient reaches its peak value and then decreases. The angle at which the lift coefficient is at its maximum value is referred to as the stall angle.

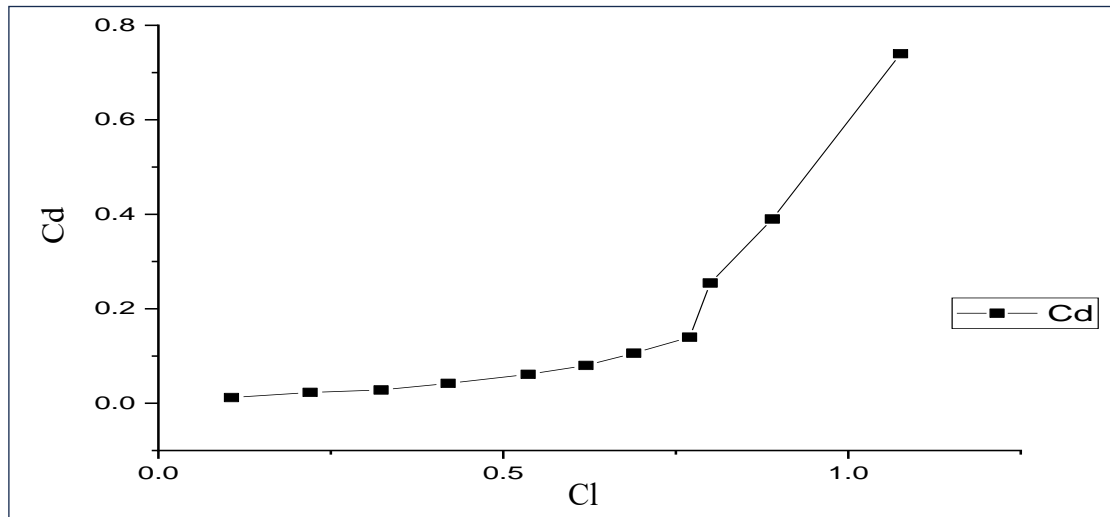


Fig. 21: Curve between Drag Coefficient and Lift Coefficient of Wind Turbine Blade

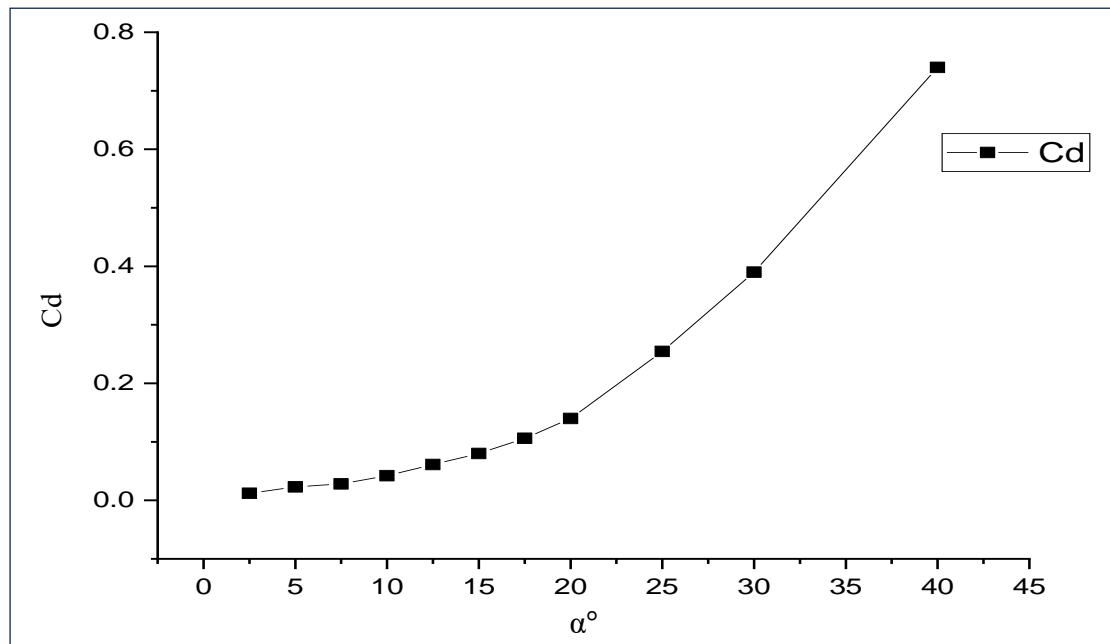


Fig. 22: Graph between Drag Coefficient and AOA

At first, the drag coefficient is zero at a zero-degree angle of attack (AOA). However, as the AOA increases, the drag coefficient gradually rises until it nears the stall angle.

Near the stall angle, the drag force increases rapidly due to the increased turbulence in the airflow.

At first, drag coefficient is slight increasing with increasing lift coefficient of the turbine blade. However, as the increasing angle of attract (AOA) after stall angle the lift coefficient increasing small amount but the drag coefficient is rapidly increasing.

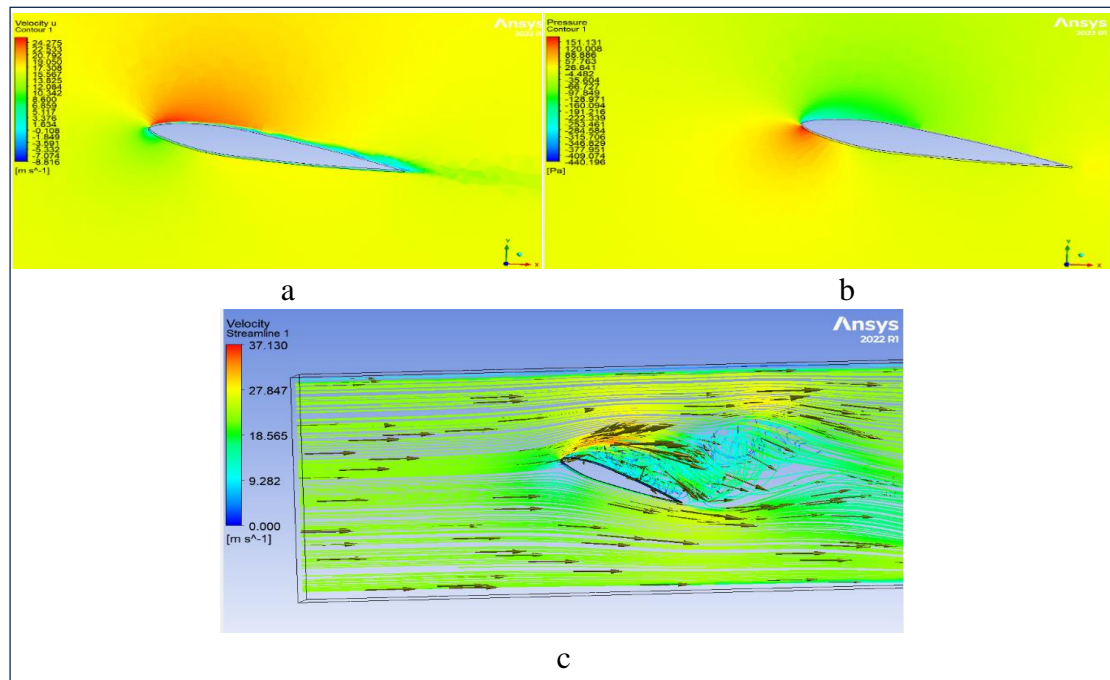


Fig. 23: a-Velocity Contour, b- Pressure Contour, c- Velocity with Streamline of wind turbine Blade Aerodynamic Analysis

Drag Force and Lift Force:

All calculations are done at 10° AOA with 60 Km/h speed of wind and 112696 Reynolds number.

Drag is a loss that must be overcome with another force, if an object is to move against a stream. The moment around this axis is called a rolling moment.

$$D_d = \frac{1}{2} \times C_d \times \rho \times w^2 \times c \times dr$$

Where,

D_d = Drag force

C_d = Drag coefficient

W = Relative air speed

C = Blade cord length

r = Blade radius

$$C_d = \frac{2 \times D_d}{\rho \times w^2 \times c \times dr} = \frac{2 \times 0.1815}{1.22 \times 16.67^2 \times 0.1 \times 0.255} = 0.04$$

This force very essential for wind turbine. The lift force can be determined as,

$$D_L = \frac{1}{2} \times C_L \times \rho \times w^2 \times c \times dr$$

Where,

D_L is the Lift Force

C_L is the Lift Coefficient

$$C_L = \frac{2 \times D_L}{\rho \times w^2 \times c \times dr} = \frac{2 \times 1.8152}{1.22 \times 16.67^2 \times 0.1 \times 0.255} = 0.42$$

Torque Coefficient (C_t): The torque coefficient is usually used to measures the performance of a wind turbine. This is given the ratio of the actual produced torque to the torque due to the force of the wind on the turbine rotor.

$$C_t = M / 0.25 \rho v^2 D_1 s$$

Where,

C_t is the torque coefficient

M is the torque (Nm)

ρ is the air density (Kg/m³)

V is the air velocity (m/s)

D_1 is the turbine outside diameter

S is the rotor swept area (m²)

$$C_t = M / 0.25 \rho v^2 D_1 s = \frac{0.0513}{(0.25 \times 1.22 \times 16.67^2 \times 0.51 \times 0.204)} = 0.00582$$

Variation of Coefficient of Wind Turbine with respect to Tip Speed Ratio:

C_p can be determined by the following formula:

$$C_p(\lambda, \beta) = c_1 \left(\frac{c_2}{\lambda_i} - c_3 \beta - c_4 \right) e^{\frac{-c_5}{\lambda_i}} + c_6 \lambda \quad [29]$$

Where,

C_p is the power coefficient of wind turbine

λ is the tip speed ratio

β is the pitch angle

Where, $c_1, c_2, c_3, c_4, c_5, c_6$ are all the constant that determined by the fan manufacturer.

For this analysis the value of constant $C_1 = 0.22, C_2 = 116, C_3 = 0.4, C_4 = 5, C_5 = -12.5$ and $C_6 = 0$.

From this graph, it said that the power coefficient of wind turbine is increasing with increasing tip speed ration. But after a certain value of λ , the C_p value will be decreasing. Also, the value of C_p decreasing with increasing pitch angle. This graph show that the power coefficient of wind turbine is maximum at the value 6 tip speed ratio with 0° pitch angle.

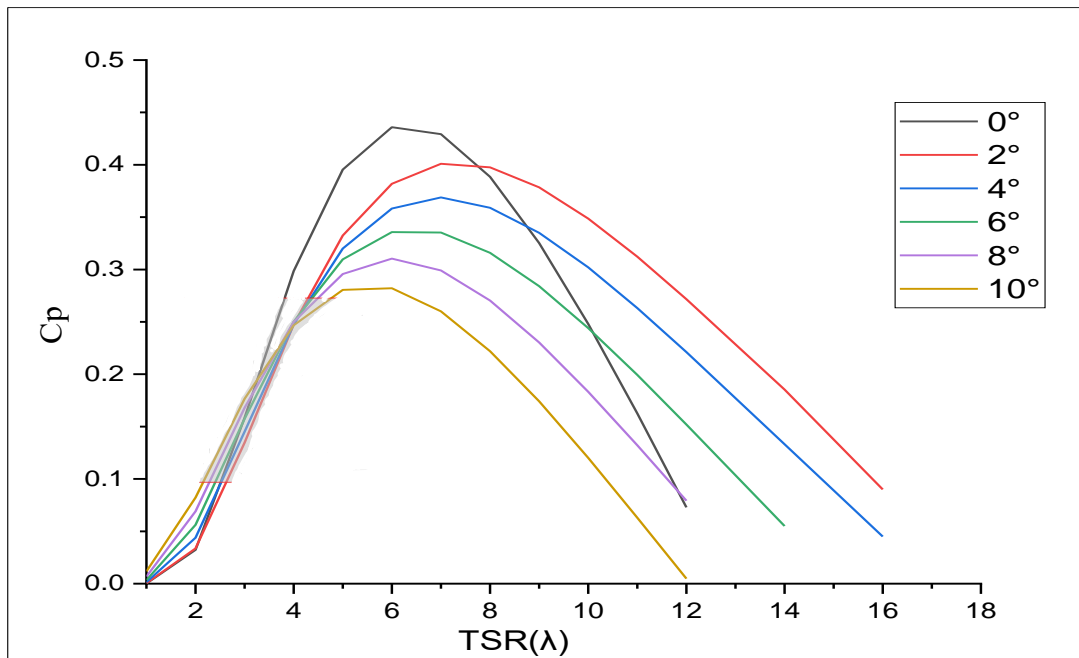


Fig. 24: Curve between Power coefficient of Turbine with Tip Speed Ratio (λ)

6.3.4 Wind Turbine Power Calculation

In hybrid vehicle design a small horizontal wind turbine is used in the frontal area of the vehicle. This small horizontal axis wind turbine CFX model has been analysed using Ansys Software 2016 and 2022 Version.

The block's output is mechanical power (P_w), which it derives from the inputs of actual and desired speeds. Equation, provides the amount of power obtained from the wind at velocity V .

$$P_w = \frac{KE}{t} = 0.5 \times \rho \times A \times V^3$$

Where,

$$\rho = \text{Air density} = 1.22 \text{ kg/m}^3$$

$$A = \text{Swept area of the wind turbine} = \pi r^2$$

$$\text{So, } A = \pi \times 0.255^2 = 0.204 \text{ m}^2$$

At 60 Km/h or 16.67 m/s, the available mechanical power for the wind turbine is

$$P_w = 0.5 \times \rho \times A \times V^3 = 0.5 \times 1.22 \times 0.204 \times 16.67^3 = 576.45 \text{ W}$$

From the wind turbine analysis, we found the value of wind turbine power ecoefficiency (C_p) is 0.26 at 16.67 m/s and at 25° angle of wind attack on the wind turbine blade.

So, the actual electrical power output from the wind turbine is,

$$P = C_p \times P_w = 0.26 \times 576.45 = 150 \text{ W}$$

At $\alpha = 05^\circ$ angle of attack wind on the wind turbine blade,

Table 5: Power output from Wind Turbine at 05° AOA

Velocity of Wind (km/h)	Power Coefficient Value (C_p)	Power output from Wind Turbine (P) (W)
30	-0.030	-2.2
40	-0.026	-4.55
50	-0.024	-8
60	-0.024	-13.9

At $\alpha = 10^\circ$ angle of attack wind on the wind turbine blade,

Table 6: Power output from Wind Turbine at 10° AOA

Velocity of Wind (km/h)	Power Coefficient Value (C_p)	Power output from Wind Turbine (P) (W)
30	0.095	6.9
40	0.094	16
50	0.105	35
60	0.107	62

At $\alpha = 15^\circ$ angle of attack wind on the wind turbine blade,

Table 7: Power output from Wind Turbine at 15° AOA

Velocity of Wind (km/h)	Power Coefficient Value (C_p)	Power output from Wind Turbine (P) (W)
30	0.15	12.3
40	0.176	30
50	0.18	60
60	0.183	106

At $\alpha = 20^\circ$ angle of attack wind on the wind turbine blade,

Table 8: Power output from Wind Turbine at 20° AOA

Velocity of Wind (km/h)	Power Coefficient Value (C_p)	Power output from Wind Turbine (P) (W)
10	0.23	0.7
20	0.23	4.95
30	0.22	16
40	0.24	42
50	0.24	81
60	0.24	139

At $\alpha = 25^\circ$ angle of attack wind on the wind turbine blade,

Table 9: Power output from Wind Turbine at 25° AOA

Velocity of Wind (km/h)	Power Coefficient Value (C_p)	Power output from Wind Turbine (P) (W)
30	0.25	43
40	0.25	91.5
50	0.27	119
60	0.259	150

At $\alpha = 30^\circ$ angle of attack wind on the wind turbine blade,

Table 10: Power output from Wind Turbine at 30° AOA

Velocity of Wind (km/h)	Power Coefficient Value (C_p)	Power output from Wind Turbine (P) (W)
30	0.24	17.9
40	0.24	42
50	0.25	84
60	0.26	150

At $\alpha = 40^\circ$ angle of attack wind on the wind turbine blade,

Table 11: Power output from Wind Turbine at 40° AOA

Velocity of Wind (km/h)	Power Coefficient Value (C_p)	Power output from Wind Turbine (P) (W)
30	0.27	20
40	0.2	35
50	0.19	66
60	0.187	108

At $\alpha = 50^\circ$ angle of attack wind on the wind turbine blade,

Table 12: Power output from Wind Turbine at 50° AOA

Velocity of Wind (km/h)	Power Coefficient Value (C_p)	Power output from Wind Turbine (P) (W)
30	0.15	11
40	0.15	26
50	0.14	49
60	0.14	83

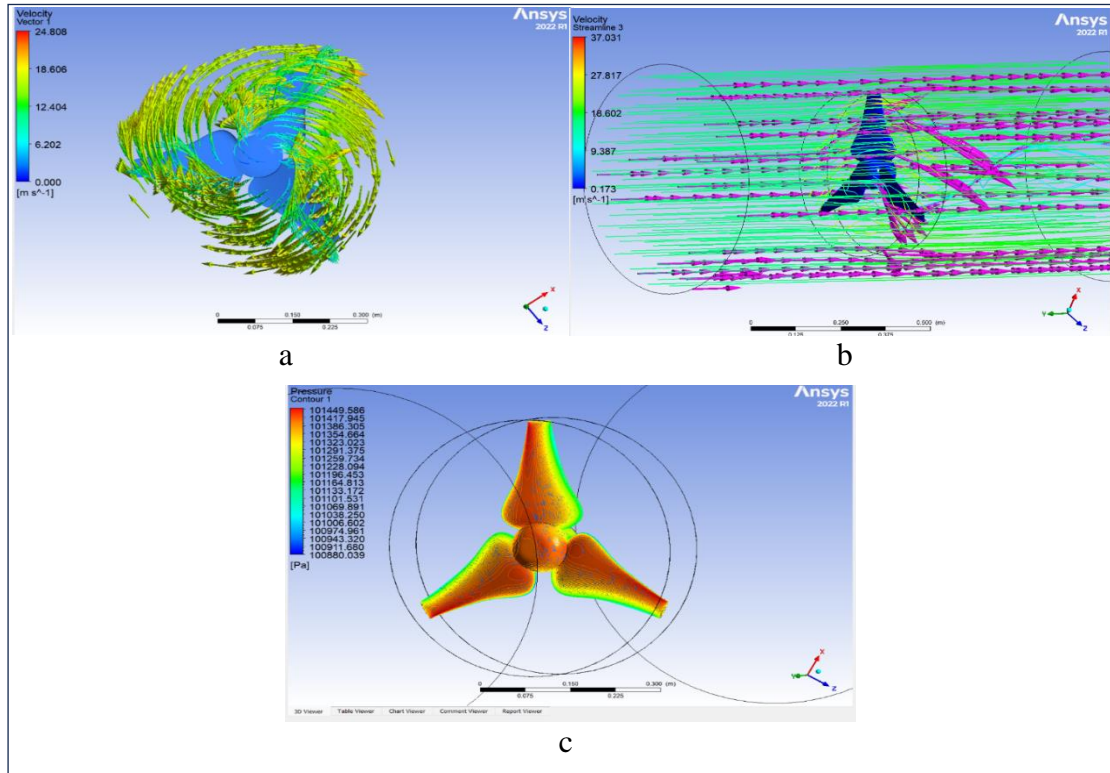


Fig. 25: a-Velocity Vector only rotation area of blade, b-Pressure Contour and c-Velocity Vector of the Wind Turbine Power Calculation

At 60 km/h wind speed we found the maximum power coefficient value (C_p) is 0.26 and the maximum power output value is 150 Wh.

Let assume that the electric vehicle run for an average of 3 hours per day. So, approximately per day power output from the designed wind turbine is $150 \times 3 = 450 \text{ W}$.

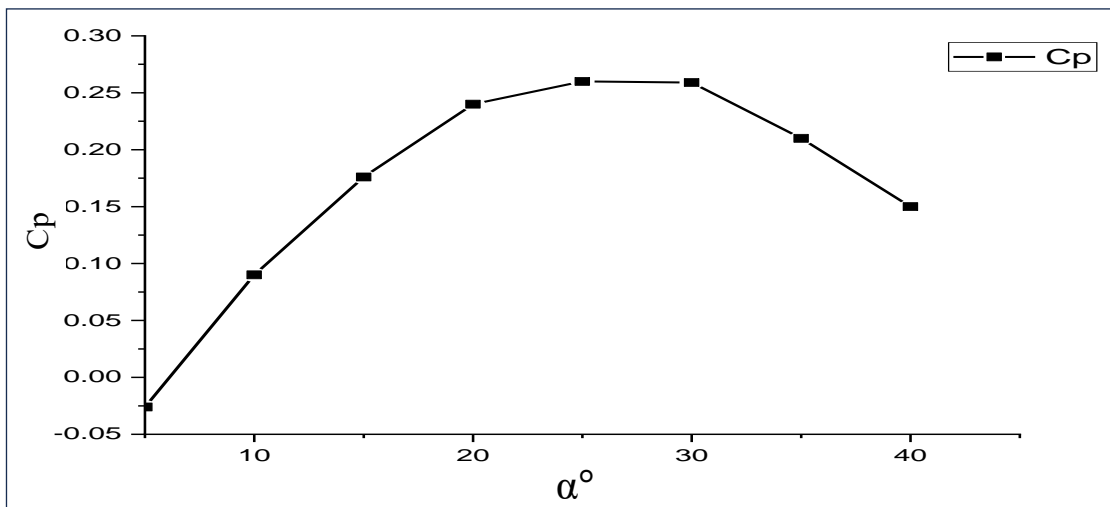


Fig. 26: Wind Turbine Power Coefficient Variation with AOA (α°)

The power coefficient (C_p) and the angle of attack (AOA) curve demonstrate that C_p increases as AOA increases. However, beyond a certain point, C_p starts to decrease. Between 20° and 30° AOA, C_p reaches its maximum at a specific relative velocity.

6.3.5 Aerodynamic Analysis of the Vehicle

A drag coefficient (C_d) is a numerical value that indicates the resistance encountered by an object moving through in a fluid. In real life, all fluids (e.g., air) have a tendency of resisting object passing through them with a force which acts opposite to the relative motion of the respective object. A minimum disturbance to the air around the vehicle is necessary to reduce its coefficient of drag. When the air strikes specific areas of the vehicle, changes direction or velocity, or is disturbed, this coefficient increases.

The drag coefficient of production cars is typically between 0.25 and 0.3, while SUVs and others big size car have a higher value at 0.35-0.45 because of their boxy appearance.

Drag is a result of the difference in pressure between the front and back of the car. At the increase the speed of a car, the pressure at the stagnation point rises along with the air's momentum, while the pressure at the back falls. As a result, the pressure difference between the front and rear of the vehicle increases as the vehicle's velocity rises.

Drag coefficient of a vehicle is obtained from the formula,

$$C_d = \frac{2 \times F}{\rho \times v^2 \times A_f}$$

Where,

F is the drag force

ρ is the air density

v is the relative velocity of the car with wind

A_f is the frontal area of the vehicle (2.36 m²)

From aerodynamic analysis of Maruti Eeco vehicle at 60 Km/h, the value of drag force is 149.951 N.

So, the value of drag coefficient is,

$$C_d = \frac{2 \times 149.951}{1.22 \times 16.67^2 \times 2.36} = 0.37$$

From aerodynamic analysis of the vehicle find that the average drag coefficient is 0.37.

From drag force vs velocity curve it can be said that the drag force of the car increasing with car velocity.

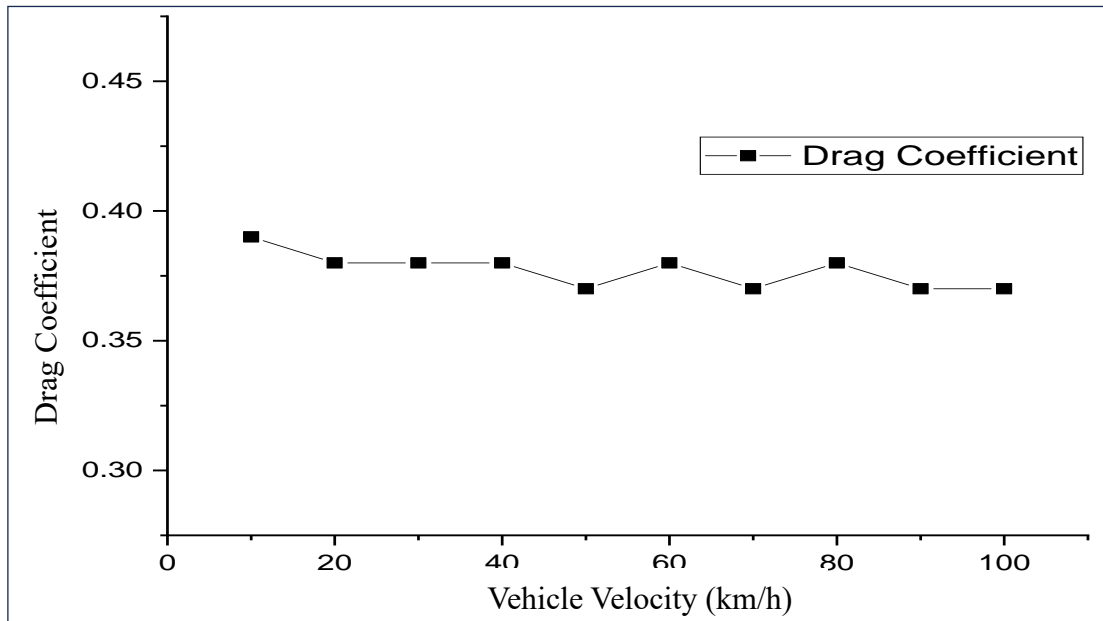


Fig. 27: Graph Between Drag Coefficient of Vehicle and Vehicle Velocity

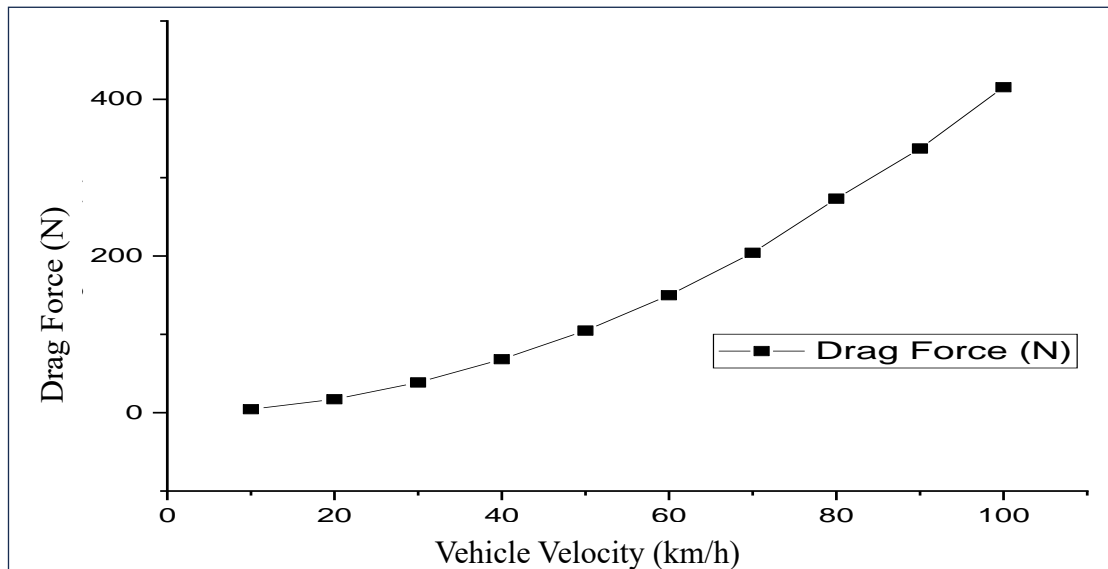


Fig. 28: Graph Between Drag force of Vehicle and Vehicle Velocity

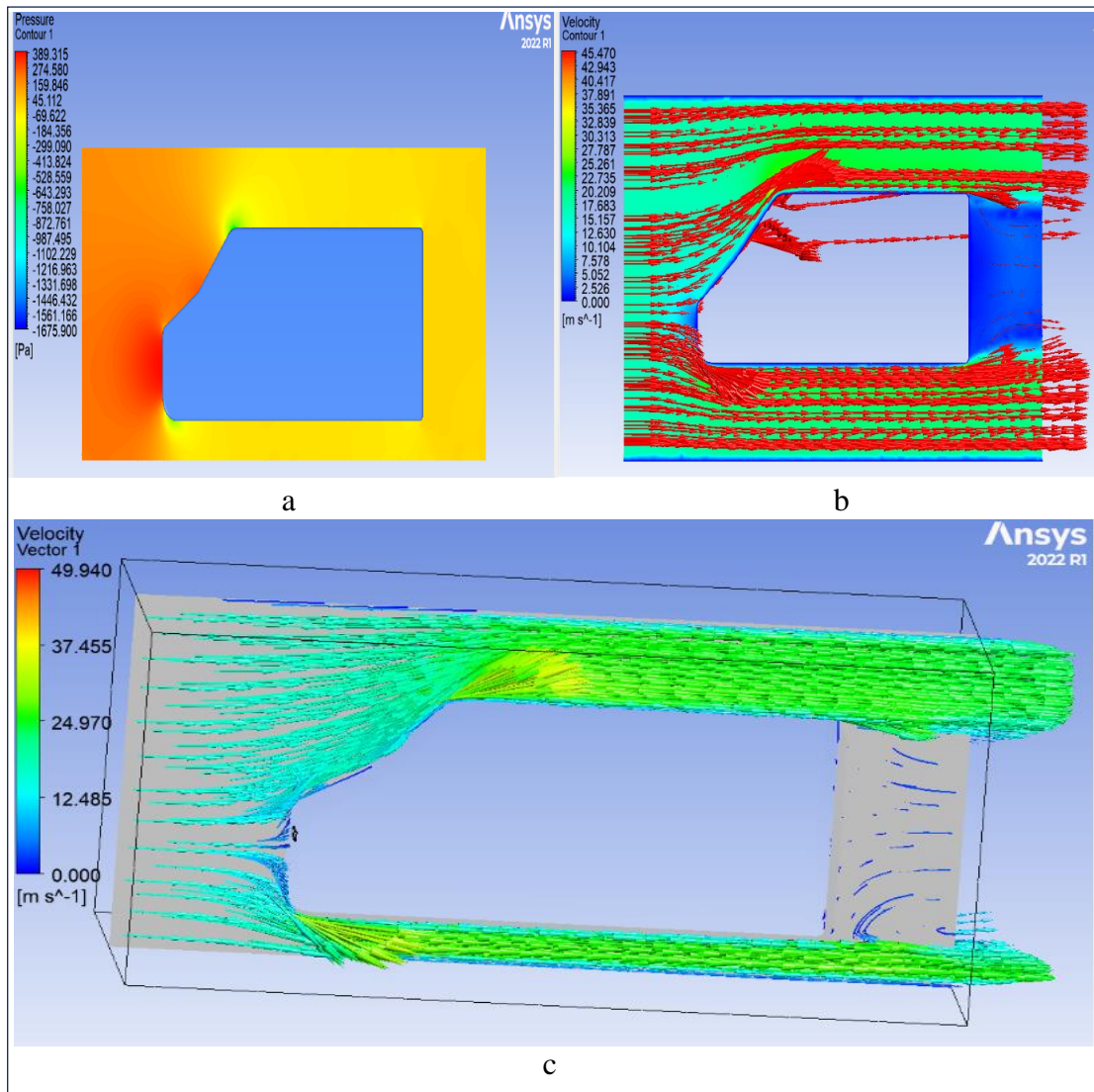


Fig. 29: a-Pressure Contour, b-Velocity Contour and c-Velocity Vector of Vehicle Aerodynamic Analysis

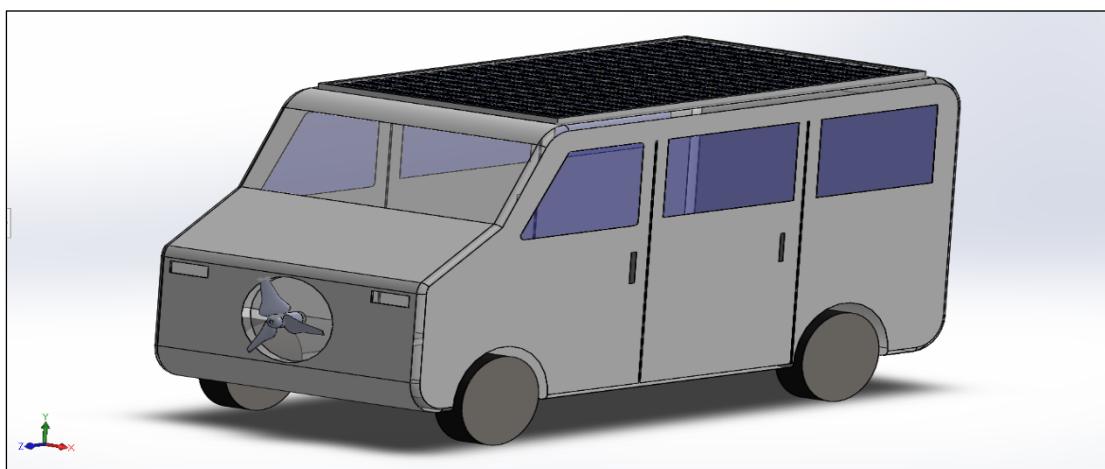


Fig. 30: Final Vehicle Design

This is the final look of designed vehicle after the solar panel and wind turbine installed.

6.3.6 Required Power Calculation for Maruti Eeco Car at 60 Km/h

Specification of Maruti Eeco 7-Seater Car:

Total weight of this vehicle is,

$$W_T = \text{Kerb Weight} + \text{Passengers Weight}$$

$$W_T = 1035 + 200 = 1235 \text{ Kg}$$

Now, Diameter of rim,

$$D_{rim} = 13 \times 25.4 = 330.2 \text{ mm}$$

$$D_{tyre} = 2 \times w \times \left(\frac{AR}{100} \right) + D_{rim}$$

Where,

W = Sectional Width of Tyre = 155 mm, AR = Aspect Ratio = 65%

Table 13: Specification of Maruti Eeco 7-Seater Car

Length (mm)	3675
Width (mm)	1475
Height (mm)	1825
Seating Capacity	7
Wheel Base (mm)	2350
Front Tread (mm)	1280
Rear Tread (mm)	1290
Kerb Weight (Kg)	935
Tyre Size	155/65 R13 LT
Wheel Size	13

$$D_{tyre} = 2 \times 155 \times \left(\frac{65}{100} \right) + 330.2 = 201.5 + 330.2 = 531.7 \text{ mm}$$

Angular Velocity of Tyre:

$$\omega = \frac{G \times v}{r}$$

Where,

G = Gear Ratio = 5

v = 16.67 m/s

$$r = \frac{D_{tyre}}{2} = 265.8 \text{ mm}$$

So,

$$\omega = \frac{5 \times 16.67}{0.2658} = 313.52 \text{ rad/s}$$

Number of tyre rotation,

$$N = \frac{60 \times 313.52}{2 \times \pi} = 2993.92 \approx 3000 \text{ rpm}$$

For the motion of an automobile, the car tractive force should be overcome to all the resistance forces. The formula of tractive force is,

$$F_T = F_w + F_r + F_g + F_a$$

Where,

F_T = Total tractive force at wheel

$$F_w = \text{Aerodynamic force} = \frac{\rho \times C_d \times A \times V^2}{2}$$

C_d is the drag coefficient of the vehicle = 0.37

A is the frontal area of the vehicle

$$\text{So, } F_w = 0.5 \times 1.22 \times 0.37 \times 2.38 \times 16.67^2 = 149.95 \text{ N}$$

$$F_r = \text{Rolling resistance force} = W \times \mu_r \times \cos \theta = 1235 \times 9.81 \times 0.014 = 169.61 \text{ N}$$

$$F_g = \text{Grade resistance force} = W \times \sin \theta$$

$$F_a = \text{Acceleration resistance force} = a \times m_i$$

Where, a is the acceleration and m_i is the inertial vehicle mass.

Assume that the vehicle is moving on a flat road and with a constant velocity. So, at this condition the component of grade resistance force and acceleration resistance force are zero.

$$\text{Total force required, } F_T = 149.95 + 169.61 = 319.56 \text{ N}$$

Now, Total power required to run the vehicle at 16.67 m/s constant speed

$$P_T = \frac{F_T \times V}{1000} = \frac{319.56 \times 16.67}{1000} = 5.3 \text{ kWh}$$

6.3.7 Battery Capacity Design

For reached required motor power a 6 kW BLDC motor is selected for this vehicle design. Efficiency of the BLDC motor is 80%. So, actual required power to run the motor is 7500 Wh.

The voltage of lithium-ion battery is 120 Volts. So, required current to run that motor is $7500 = 120 \times I$

$$I = 62.5 \text{ Ah} = 63 \text{ Ah}$$

To run the 7500 Wh motor for 1 hour a 120 V and 63 Ah lithium-ion battery is required. So, if a vehicle is moving at average speed of 60 km/h with 120 V and 63 Ah lithium-ion battery provided 60 km mileage. Now, this vehicle design for 160 Km milage at one time full charge of battery pack.

Current fluctuation factor is 0.95, so net current value is 66.31 A.

Actual energy required to run the vehicle $E = V \times I = 120 \times 66.31 = 7.95 \text{ kW}$.

For 200 km millage total required energy capacity of the battery pack is

$$= \frac{7.95 \times 160}{60} = 21.2 \text{ kW}$$

Average lithium-ion battery efficiency is 0.85. So actual required battery capacity is

$$\frac{21.6}{0.85} = 24.9 \text{ kW} = 25 \text{ kW}.$$

6.3.8 Cost and Weight Analysis

Table 14: Components Details of Designed Vehicles

Designed Electric Vehicle Products Details	Weight (kg)	Cost
450 Wp Half Cut 144 Cells Monocrystalline Solar Panel	25	18.56 k
Solar MPPT Charge Controller	15	20 k
Wind Turbine	6	5 k
Motor Controller	17	45.43 k
6 kW 120 V BLDC Motor	13	43.129 k
Lithium-ion Battery	200	216 k
Differential		20 k
Foot Throttle		2 k

Modification		20 k
Charger	2-3	15 k
Generator	11	16 k
Total	290	421.199 k

Component removed from Vehicle:

Table 15: Details of removed component of Vehicle

Name of Components	Weight (Kg)	Cost
Engine	180	80 k
Fuel Tank	4-5	3 k
Crank shaft		20 k
Muffler		8.16 k
Controller of fuel injector		7.565 k
Exhaust pipe		35.93 k
Oxygen Sensor		2.36 k
Shroud		0.84 k
Others Parts	10	10-15 k
Total	195	172.875 k

From this cost and weight analysis, it is evident that total weight increases by approximately 100 kg and total cost by approximately ₹230 k.

Chapter 7

Results & Discussion

7.1 Solar and Wind Energy Resource Assessment Results

From the designed monocrystalline solar panel value of average solar energy incident is 1000 W/m^2 at a particular time. So, the annually average total amount of solar radiation energy incident on this solar panel is 3900 Watts at a particular time. From the analysis it is found that the overall efficiency of the designed solar panel is 15.18%. So, the average total amount of electric energy produced by the solar panel is 430 Watts per hour. Now, total amount of electric energy produces is 3.38 kW per day.

From the analysis it is find that the value of power coefficient of the designed horizontal wind turbine is 0.26 and average power output is 450 W per day.

7.2 Design and Integration Results

7.2.1 Solar Panel Result

The analysis demonstrates the promise of renewable solar energy as a significant electrical source. During midlatitude summer, the monocrystalline PERC solar panel generates 3.38 kW of electric energy per day. The overall efficiency of this solar panel design stands at 15.8%.

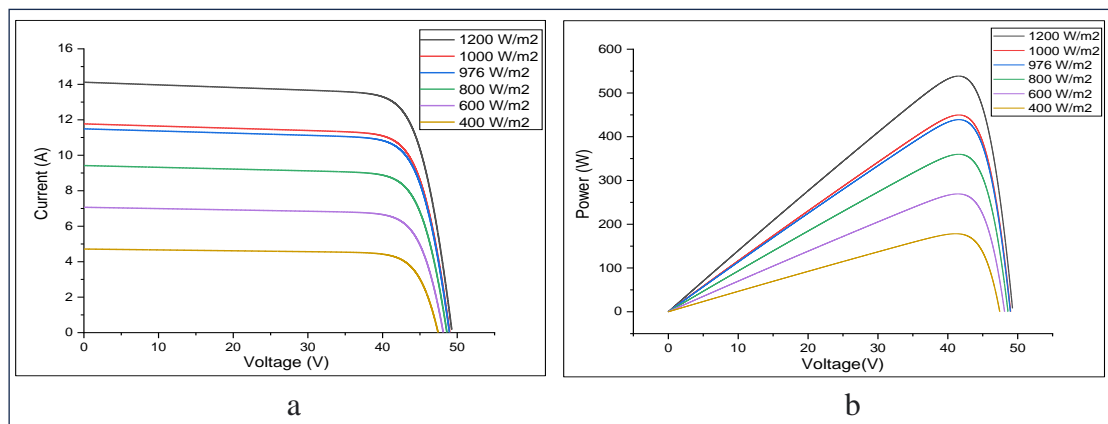


Fig. 31: At constant 25°C Temperature a-Output Current and b-Output Power Vs. Voltage Curve of Solar Panel at Different Solar Radiation Energy

This is a curve of output voltage vs current and power at different solar irradiation on the design solar panel at 25°C. From this curve it is said that the output power and output current with respect to output voltage increasing with increasing solar irradiation value. At 1000 W/m² solar irradiation the output voltage, current and power are 41.52 Volts, 10.88 Amperes and 449.7 Watts respectively.

This is a graph plot of output voltage vs power and current at different temperature (°C) of design solar panel with at constant solar irradiation 1000 W/m². From this curve it is said that the output power and output current increasing with decreasing solar panel average temperature. As a result, the solar panel works best when it's cold atmospheric. At standard temperature 25°C the output voltage, current and power are 41.52 Volts, 10.87 Amperes and 449.7 Watts respectively.

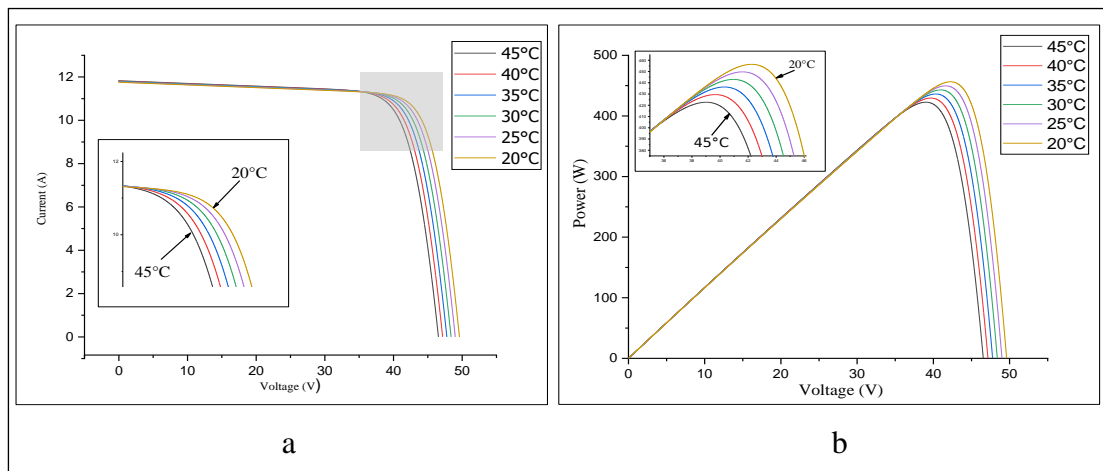


Fig. 32: At constant 1000 W/m² Irradiance a-Current and b-Power Vs. Voltage Curve of Solar Panel at Different Atmospheric Temperature

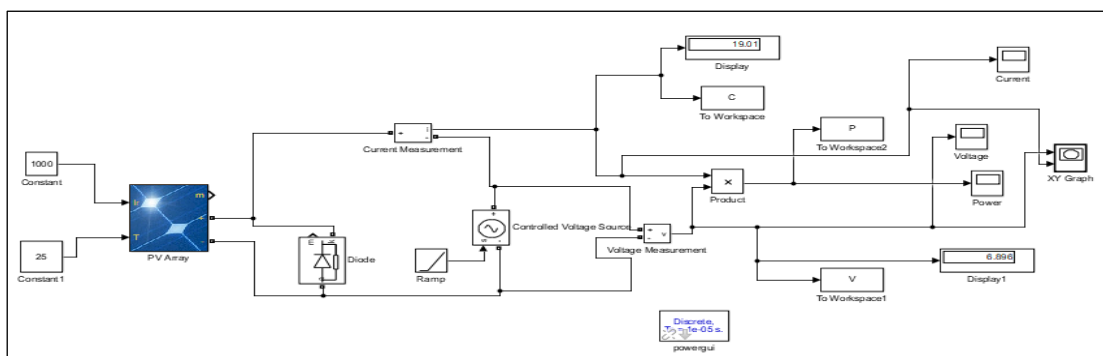


Fig. 33: MATLAB simulation model of Solar Panel Analysis

This is the MATLAB simulation model for the solar panel analysis.

7.3 Performance Analysis Results

From the analysis, it is found that at low atmospheric temperature performance of solar panel is increasing. In solar panel efficiency analysis, the solar cell efficiency calculation formula is,

$$\eta_s = 0.28 - 0.001(T_{\text{cell}})$$

Where, T_{cell} is the average temperature of solar cell and calculate from ANSYS simulation.

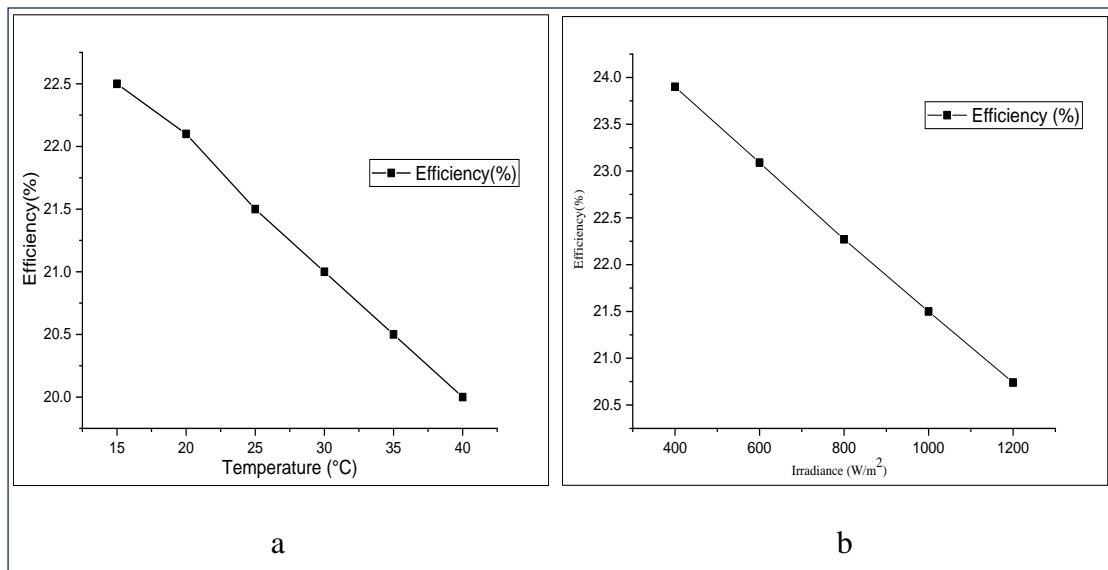


Fig. 34: a-Variation of Solar Panel Efficiency with Temperature at 1000 W/m² Irradiance and b-Variation of Solar Panel Efficiency with Solar Irradiance at 25°C Temperature

The graph illustrates a crucial relationship between the efficiency of a solar panel and the atmospheric temperature. It demonstrates that as the atmospheric temperature increases, the efficiency of the solar panel decreases. In other words, when it gets hotter outside, the solar panel becomes less effective at converting sunlight into electricity. This decrease in efficiency with rising temperatures is a well-documented phenomenon in solar energy systems. One of the key reasons behind this effect is that most solar cells and modules become less efficient as the temperature rises. This is often referred to as the temperature coefficient of solar panels.

The explanation for this phenomenon lies in the behaviour of semiconductor materials within the solar cells. As the temperature increases, the electrons in these materials become more excited and more energetic. This higher energy state can make it more difficult for the solar cells to efficiently capture and convert the incoming photons from sunlight into electrical energy. Consequently, the overall efficiency of the solar panel drops.

The statement also provides a practical insight into the impact of temperature on solar panel performance. It mentions that for every five degrees Celsius (or approximately nine degrees Fahrenheit) increase in temperature above 25°C (77°F), the output power of the solar panel decreases by about half of a percent. This means that if the temperature were to rise significantly above 25°C, the solar panel's efficiency would progressively decline, potentially affecting its ability to generate electricity at its maximum capacity. Understanding these temperature-related effects is crucial for designing and optimizing solar energy systems, as it allows for better management of the system's performance under varying environmental conditions. It also emphasizes the importance of cooling or temperature management strategies to mitigate the negative impact of high temperatures on solar panel efficiency.

From the graph 34(b) between efficiency of solar panel and solar irradiance it is find that the efficiency is decreasing with increasing of solar irradiance value.

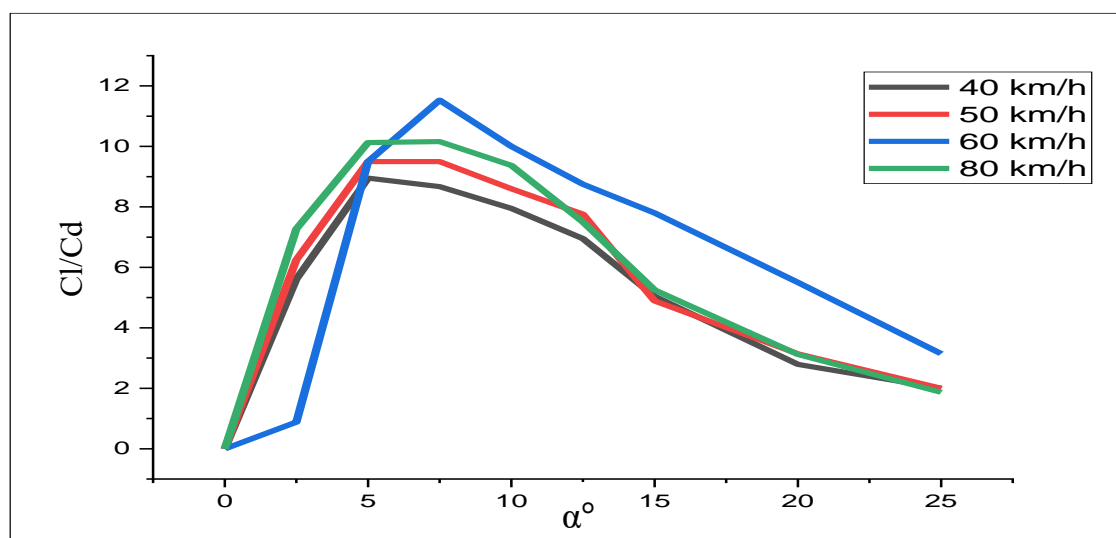


Fig. 35: Value of C_l/C_d change with AOA(α°) at Different Vehicle Speed

The graph about C_l/C_d and angle of attack tells us that when the wind turbine is at an angle of 7.5 degrees, with a Reynolds number of 112696, and a wind speed of 60 km/h, it has the highest C_l/C_d value, which is 11.53. This means that at this specific condition, the lift force on the wind turbine blade is 11.53 times stronger than the drag force. In simpler terms, the wind turbine operates most efficiently when the vehicle is moving at 60 km/h in relation to the wind.

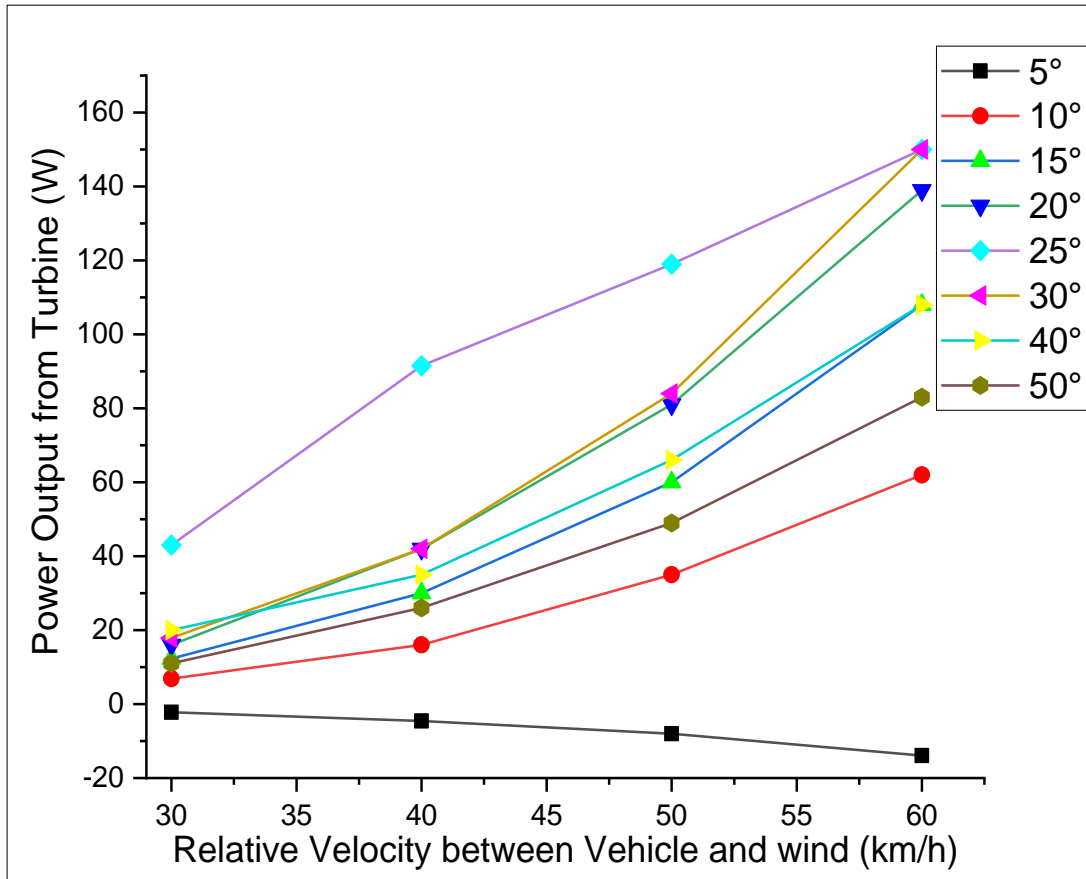


Fig. 36: Wind Turbine Output Power with Relative Velocity between vehicle and wind at Different AOA

Analysing this curve further, it becomes evident that the designed wind turbine achieves its highest output power within the angle of attack (AOA) range of 20° to 30°. At a relative speed of 60 km/h and with the turbine blades operating in this AOA range, the maximum power output reaches 150 Watts. It's noteworthy that within this AOA range, the curve closely aligns with the theoretical power output curve expected from a horizontal axis wind turbine.

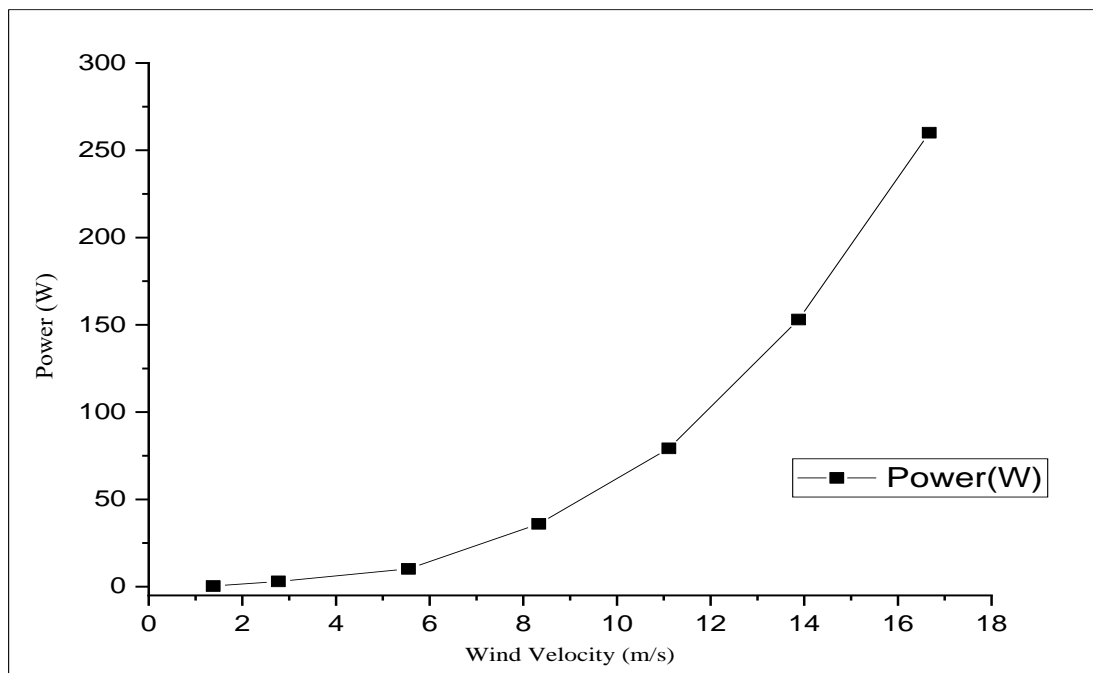


Fig. 37: Curve of Wind Turbine Power Vs. Wind Velocity

From this curve said that the output power from wind turbine is very small up to 5.55 m/s wind speed, but after this range of wind velocity the power output is increasing rapidly.

7.4 Discussion of Findings

Table 16: Table of Wind and Solar System Simulation and Analysis Result

Total Tractive Force Required	5.3 kW
Total Power Consumption by the Design Car at run 60 Km/h	7.95 kW
Energy Output from the Designed Solar Panel	3.38 kW
Energy Output from the Designed Wind Turbine per Day	450 W
Battery Capacity	25 kW
Efficiency of Solar Panel	15.6 %
Power Coefficient of the Wind Turbine	0.26
Total Energy Generation by Solar and Wind Hybrid System	3.83 kW/per day

The analysis indicates that the hybrid solar and wind energy system integrated into the vehicle can contribute significantly to its energy needs. Specifically, this system is capable of generating approximately 14-15% of the total energy capacity of the

vehicle's battery. To put this into perspective, if we consider the vehicle's battery as a whole, this hybrid system can provide around 14-15% of the energy it can store. This is a notable contribution because it means the vehicle can rely on renewable energy sources to supplement its power requirements, reducing its dependence on conventional energy sources and, potentially, its environmental footprint.

Furthermore, on an annual basis, the solar and wind renewable energy system produces an average of 3.83 kilowatts (kW) per day. This figure represents the combined daily energy output from both the solar panels and wind turbine over the course of a year. It highlights the system's ability to consistently generate renewable energy, which can be harnessed to power the vehicle and reduce its reliance on non-renewable energy sources. This reduction in fossil fuel consumption can have positive environmental impacts by reducing greenhouse gas emissions and promoting sustainable energy practices.

Chapter 8

Conclusion and Future Work

8.1 Summary of Findings

This paper presents the successful creation of a hybrid vehicle that combines solar and wind power with Plug-In Electric Vehicle (PHEV) technology. Electric hybrid vehicles often face challenges during long trips and need frequent battery recharges. To address these issues, we integrated a hybrid solar and wind power system into the vehicle, harnessing renewable energy sources. This innovation allows the vehicle to self-charge via solar panels and a wind turbine.

The solar panel used in this system has an efficiency of 15.18%. Although the cost of the hybrid solar-wind-plug-in vehicle surpasses that of traditional vehicles, it offers heightened efficiency, reduced noise, increased eco-friendliness, and a complete lack of pollution. The solar and wind energy systems are interconnected in series to maximize their potential. The combined energy output of this hybrid system is 3.83 kW. This hybrid solar wind system can produce 14-15% of total battery capacity energy.

For an hour of driving at 60 km/h, the Maruti Eeco car typically requires about 7.95 kW of electric power from a battery. As a result of our hybrid solution, the solar and wind hybrid electric vehicle can autonomously cover approximately 29 km each day without relying on conventional energy sources.

8.2 Contributions to Sustainable Transportation

However, energy production is essential for human survival and social progress. Finding energy without harming the environment is the biggest problem society is currently facing in the twenty-first century. The issue is fixed by utilizing renewable energy sources. Solar and Wind energy are the greatest example of sustainable energy sources. Wind energy and solar energy are a sustainable, clean, and renewable energy sources that can be an alternative energy source to fossil fuels. Utilizing sustainable

energy is essentially based on its capacity to lower emissions of greenhouse gases and pollution.

8.3 Limitations and Challenges

After going through the literature review, we come to know that the blade design of the wind turbine is the most complex part to produce a wind turbine system. The design is unattractive when a wind turbine is attached to a car. The car's design plays a significant role in our decision when it comes time to purchase a vehicle. If the hybrid car is unattractive to look at, it won't be well received by everyone. Perhaps solar and wind power will be used in the future to produce a more aesthetically pleasing car model.

After some time period the charging control system and the battery system losing their efficiency. After some time period the battery is take more time to recharge and gives less backup. In the future, there will be more research on increasing the efficiency of charging system and battery system. Also, the battery set is much heavier which reduces the overall efficiency of the vehicle. In future, there will be lot of research on to make more compact, lightweight and high-capacity batteries.

Solar panels are the most promising renewable energy source for an eco-friendly EV. But the solar panel could only be used during the day. Therefore, this solar panel system has a negative impact on the vehicle's efficiency at night times.

8.4 Future Research Directions

In the future solar energy and wind energy will play a massive role to fulfil the energy crisis. Now a day solar energy converted into useful electric energy by solar panel. However, due to their current efficiency, solar panels cannot be used to power an electric vehicle that uses only solar power system. So, in future a lot of research in going on to increasing the efficiency of the solar panel.

In future designed electric vehicle of solar and wind energy system with regenerative braking system and regenerative suspension system. This combination of hybrid vehicle can make a huge role to create an eco-friendly vehicle.

In future research on vehicle wind power system with vertical axis wind turbine installed on the roof top parallel or vertically to the roof top surface.

The weight of the battery pack is much heavier which might have a negative effect on the vehicle's overall efficiency. We are well aware of the limitations imposed on the current lithium-ion batteries used to power EVs. While computer chips and operating systems continue to advance in saving power, battery packs have been the weak link, until now. However, a number of fresh battery technologies are currently being developed, such as lithium-ion batteries with silicon anodes, cobalt-free lithium-ion batteries, and batteries with carbon nanotube electrodes.

The automotive industry is undergoing a revolution thanks to electric vehicles, hybrid electric vehicles, and other similar automobiles. Over the next few years, these innovations will completely replace the current conventional vehicle systems. The solar and wind power industries are major contributors to this revolution. Due to the rapid advancement of technology, research and development in this area are very much needed.

References

1. M. Premkumar, JSV. Sivakumar, R.V. Krushna & R. Sowmay, "Design, analysis and fabrication of solar PV powered BLDC hub motor driven electric car". 2018. 8(1): p. 1255-1270.
2. A. Singh, S.S.Shaha, Nikhil P G, Y. R. Sekhar, S. Saboor & A. Ghosh, "Design and Analysis of a Solar-Powered Electric Vehicle Charging Station for Indian Cities. World Electric Vehicle Journal (MDPI), 2021. 12(3). <https://doi.org/10.3390/wevj12030132>.
3. G.R. Chandra Mouli, P.Bauer & M.Zemen., "System Design for A Solar Powered Electric Vehicle Charging Station for Workplaces. ELSEVIER, Applied Energy (Elsevier), 11 Feb 2016, 168: p. 434-443.
4. P. S. Sahu, A.Kumar & C.M.Bajpai, "Design Analysis and Theoretical Study of Solar Energy Conversion in an Electric Car". International Research Journal of Engineering and Technology (IRJET), 2016. 03(05): p. 1146-1150.
5. S. Maitreya, H. Singh Dangi, N.Singh Naruka & P.Paliwal, "Analysis of Solar Powered Electric Vehicles". IEEE 2nd International Conference on Electrical Power and Energy Systems (ICEPES), 2021: p. 1-4. DOI: 10.1109/ICEPES52894.2021.9699596.
6. E. Kaleeswaran & S. Manivannan, "Solar Powered Electric Vehicle". Institute of Electrical and Electronics Engineers (IEEE). 2016. <https://doi.org/10.1109/SGBC.2016.7936074>.
7. Alani, W., et al., Enhancing the fuel saving and emissions reduction of light-duty vehicle by a new design of air conditioning worked by solar energy. 2022. 30: p. 101798.
8. M. Awad, A.M. Ibrahim, Z.M. Alass, A. El-Shahat & A.I. Omar, "Design and analysis of an efficient photovoltaic energy-powered electric vehicle charging station using perturb and observe MPPT algorithm". 2022. 10: p. 969482. <https://doi.org/10.3389/fenrg.2022.969482>.

9. Z. Jin, D. Li, D. Hao, Z. Zhang, L. Guo, X. Wu & A.Y. yuan, "A portable, auxiliary photovoltaic power system for electric vehicles based on a foldable scissors mechanism". 2024. 5(1): p. 81-96. <https://doi.org/10.1016/j.enbenv.2022.08.002>.
10. Y. Ota, K. Araki, A. Nagaoka & K. Nishioka, "Facilitating vehicle-integrated photovoltaics by considering the radius of curvature of the roof surface for solar cell coverage". 2022. 7: p. 100446. <https://doi.org/10.1016/j.clet.2022.100446>.
11. P. W. Ripley, H.W.U., Wind Turbine for Electric Car. United States Patent, 2019. Patent, Patent No: US 10,358,038 B1.
12. Kajal, A. Gulhane, "Design And Implementation Of Vehicle Wind Turbine". International Conference On Digital Society, Innovation & Integration Of Life In The New Century (ICDSIIL), E-ISSN. 2020.
13. L. Mishnaevsky, K. Branner, H.N. Petersen. J. Beauson, M. Mc Guban & F. Bent "Materials for wind turbine blades: An overview". 9 November 2017. 10(11): p. 1285. doi:10.3390/ma10111285.
14. F.T. Weng & Y.X. Huang. " An Investigation of Vehicle Wind Turbine System " IEEE International Conference on Applied System Invention (ICASI). 2018. IEEE.
15. E. El, C. Ildiz, B. Dandil & A. Yildiz. " Effect of wind turbine designed for electric vehicles on aerodynamics and energy performance of the vehicle". Thermal Science: Year 2022, Vol. 26, No. 4A, pp. 2907-2917. <https://doi.org/10.2298/TSCI2204907E>.
16. G.R. Chandra Mouli, P. Bauer, & M. Zeman, "System design for a solar powered electric vehicle charging station for workplaces". ELSEVIER, Applied Energy 168 (2016) 434-443, 11 Feb 2016.
17. Z. Belfkira, H. Mounir & A. El Marjani, "Structural optimization of a horizontal axis wind turbine blade made from new hybrid composites with kenaf fibers". 2021 Mar 15; 260: p. 113252.
18. A. Gupta, & N. Kumar, "Energy regeneration in electric vehicles with wind turbine and modified alternator". Materials Today: Proceedings. 2021. 47, Part 11, p. 3380-3386. <https://doi.org/10.1016/j.matpr.2021.07.164>.

19. A.M. Abdelsalam, W.A. El-Askary, M.A.Korb & I.M. Sakr, "Computational analysis of an optimized curved-bladed small-scale horizontal axis wind turbine". *Journal of Energy Resources Technology*. 2021 June 1. 143(6): p. 061302. DOI: 10.1115/1.4048531.
20. K.S. Rao, A. Srinath & G.B. Rao. "Design and analysis of an autonomous hybrid vehicle" . AIP Conference Proceedings. 2021. AIP Publishing.
21. A. Tekle " Renewable energy use for continuous electric vehicles battery charging capacity in mobile". *Innovative Systems Design and Engineering* www.iiste.org, ISSN 2222-1727 (Paper) ISSN 2222-2871 (Online) Vol.5, No.10, 2014.
22. T.Vignesh, S. Sathishkuma & D.Silambarasan, "Design of Hybrid Electric Vehicles Using Solar and Wind Energy with Arduino Processor". *International Journal of Advanced Research in Electrical, Electronics and Instrumentation Engineering*, 2017. 6(3): p. 9. DOI:10.15662/IJAREEIE.2017.0603075.
23. Md. Arefin, & A. Mallik, "Numerical investigation of solar and wind energy assisted plugged in hybridized engine driven autorickshaw/three-wheeler". *AIMS Energy*, 2018. 6(2): p. 358-375. DOI: 10.3934/energy.2018.2.358.
24. T. Jayaraj, P. James, R. Joy & L. James, "Hybrid Solar And Wind Powered Electric Vehicle Using Sepic Converter". 3rd International Conference on Inventive Computation Technologies (ICICT). 2018. IEEE.
25. W.A. Eltayeb, J. Somlal, S. Kumar & S.K. Rao, "Design and analysis of a solar-wind hybrid renewable energy tree". *Results in Engineering*, May 1, 2023. 17: p. 100958. <https://doi.org/10.1016/j.rineng.2023.100958>.
26. H.G. Teo, P.S. Lee and M.N.A Hawlade, "An active cooling system for photovoltaic modules". *Applied Energy*, ELSEVIER, 2012. 90(1): p. 309-315. <https://doi.org/10.1016/j.apenergy.2011.01.017>.
27. S. Dubey, G.S. Sandhu and G.N. Tiwari, " Analytical expression for electrical efficiency of PV/T hybrid air collector". *Applied Energy*, Volume 86, Issue 5, May 2009, Pages 679-705, ELSEVIER.
28. B.N. Prasad and J.S. Saini, "Optimal thermohydraulic performance of artificially roughened solar air heaters. *Solar Energy*, ELSEVIER, 1991. 47(2): p. 91-96. [https://doi.org/10.1016/0038-092X\(91\)90039-Y](https://doi.org/10.1016/0038-092X(91)90039-Y).

29. Zhi-jun Guo & X-yu Kang, "Modeling and Analysis of Vehicle with Wind-solar Photovoltaic Hybrid Generating System". Henan University of Science and Technology, Luoyang, China. (ICSEEE) 2015, ResearchGate, 2016: p. 5. [https://doi.org/10.1016/0038-092X\(91\)90039-Y](https://doi.org/10.1016/0038-092X(91)90039-Y).
30. ISRO Solar Calculator.